

- Arc stability analysis of twin-wire welding using wavelet energy entropy-

Mrityunjay kumar

Roll No-ME13M1024

A Dissertation Submitted to
Indian Institute of Technology Hyderabad
In Partial Fulfillment of the Requirements for
The Degree of Master of Technology.

Adviser-Dr. Abhay Sharma



भारतीय प्रौद्योगिकी संस्थान हैदराबाद
Indian Institute of Technology Hyderabad

Department of Mechanical and aerospace Engineering

July, 2015

Declaration

I declare that this written submission represents my ideas in my own words, and where others' ideas or words have been included, I have adequately cited and referenced the original sources. I also declare that I have adhered to all principles of academic honesty and integrity and have not misrepresented or fabricated or falsified any idea/data/fact/source in my submission. I understand that any violation of the above will be a cause for disciplinary action by the Institute and can also evoke penal action from the sources that have thus not been properly cited, or from whom proper permission has not been taken when needed.



(Signature)

Mrityunjay kumar

ME13M1024

Approval Sheet

This thesis entitled – **Arc stability analysis of twin-wire welding using wavelet energy entropy** – by – **Mrityunjay kumar** – is approved for the degree of Master of Technology from IIT Hyderabad.



Dr. Bharat Bhooshan Panigrahi

Department of Materials Science and Metallurgical Engineering

IIT Hyderabad

Chairman



Dr. S. Surya Kumar

Department of Mechanical and Aerospace Engineering

IIT Hyderabad

Examiner



Dr. Abhay Sharma

Department of Mechanical and Aerospace Engineering

IIT Hyderabad

Adviser

Acknowledgements

I would like to express my sincere thanks to my adviser Dr. Abhay Sharma for his constant support throughout my thesis work. His logical way of thinking and enthusiastic support motivated me a lot to do this project. The discussions that I had during group meetings with him were a major source of learning and improving my knowledge and communication skills. His guidance helped me all the time during the project.

I would like to thank Department of Mechanical and Aerospace Engineering, IIT Hyderabad for providing all the necessary facilities during the research work.

I am grateful to Syed Quadir, Jose MJ and Nilanjan Banerjee for sharing of knowledge and helping me a lot in my thesis work. I would like to thank my friends Bandari Vijendra, Somasekhara and Jayaprakash sharma for their co-operation and generous help throughout my project. I would like to thank Raj Kiran and Ramesh for helping me in the manufacturing and metrology lab.

I would like to express my heartfelt thanks to all my classmates and my friends for giving me the moral support.

Dedicated to

Abstract

The broader aspect of this work is to convey newer observations in twin-wire gas metal arc welding. In the prior works, it has been observed that the dissimilar currents in lead and trail leads to stabilize the arc. The present work suggests that dissimilar current density in the two electrodes can also help with arc stability, resulting into a considerable influence on HAZ Hardness and aspect ratio. If the difference of current density in the lead and trail is more, the arc attains maximum stability. With the help of dissimilar wire diameter electrodes we can achieve a higher current density difference in lead and trail.

Keywords: Twin-wire welding, Arc stability, Current-voltage signals, HAZ Hardness, Wavelet energy entropy, Aspect ratio.

Nomenclature

I_L	Lead current
I_T	Trail current
V	Voltage
I	Current
I_L	Lead Current
I_t	Trail Current
$\psi(t)$	Mexican Hat wavelets
f_b	The Bandwidth parameter
f_c	the wavelet center frequency
$G(f)$	The Fourier transform of $g(t)$
$\Delta\tau$	Time resolution
Δf	Frequency resolution
f_n	Discrete frequency component
ψ_M	Morlet wavelet
ψ_b	B-spline wavelet
ψ_s	Shannon wavelet
$P(X)$	Probability mass function of X
$I(X)$	Information of X
$H(X)$	Entropy of X
H_{Shannon}	Shannon entropy
$R(s)$	Energy to Shannon Entropy ratio
(P_{avg})	Average power
$wt(s, \tau)$	Wavelet transform of a signal $x(t)$
$\psi^*\left(\frac{t-\tau}{s}\right)$	The scaled Base wavelet
$\Psi(f)$	The Fourier transform of “ f ”
W_{EE}	Wavelet energy entropy

Abbreviation

GMAW	Gas Metal Arc Welding
TW-GMAW	Twin wire gas metal arc welding
DE-GMAW	Double electrode gas metal arc welding
TESAW	Twin wire single arc welding
HAZ	Heat affected zone
AWS	American welding society
TIME	Transferred ionized molten energy
CTWD	Contact-Tube-to-Work piece-Distance
SAW	-Submerged Arc Welding
TESAW	Twin Electrode Single Arc Welding
MRA	Multi-resolution Analysis
MS	Mild Steel
MIG	Metal Inert Gas
MAG	Metal Active Gas
GFR	Gas Flow Rate
GTAW	Gas Tungsten Arc Welding
EMI	Electro-Magnetic Interaction
DCEN	Direct Current Electrode negative
DCEP	Direct Current Electrode Positive
WEE	Wavelet energy entropy

Contents

Declaration	ii
Approval Sheet	iii
Acknowledgements	iv
Abstract	vi
Nomenclature	vii
Abbreviation	viii
1 Introduction	1
1.1 GMAW and Twin wire GMAW	1
1.2 Arc stability and previous assumptions	4
1.3 Motivation	5
2 Literature review	7
2.1 Birth and evolution of twin wire welding	7
2.2 Review of twin wire welding	8
2.3 Review on arc stability	13
2.4 Gaps and opportunities	17
3 Objective and methodology	19
3.1 Problem statement	19
3.2 Objective	19
3.3 Methodology	20
4 Experimental procedure	21
4.1 Selection of material and process parameters	24
4.1.1 Selection of material	24
4.1.2 Process parameters	25
4.2 Welding of the work-piece	27

4.3	Data Acquisition	28
4.4	HAZ Hardness and weld bead geometry measurement	28
5	Wavelet transform	31
5.1	Introduction of Wavelet transform	31
5.2	Roles of signal processing in welding	32
5.3	A Historical prospective of the wavelet transform	34
5.3.1	Fourier transform	34
5.3.2	Short-time Fourier transfor	35
5.3.3	Wavelet transform	36
5.4	The wavelet transformation of the signal	37
5.4.1	Continuous Wavelet Transform(CWT)	37
5.4.2	Discrete wavelet transform (DWT)	41
5.5	Selection of base wavelet	43
5.5.1	Qualitative approach	43
5.5.2	Quantitative approach	46
5.6	Entropy of a signal	47
5.7	Energy of a signal	49
5.8	Wavelet energy entropy (WEE)	50
5.9	Criteria for the wavelet selection	51
6	Results and discussion	52
6.1	Wavelet analysis	52
6.1.1	Criteria for wavelet selection	52
6.1.2	Signal Entropy analysis	55

6.1.2.1	Comparative study of arc stability for equal and unequal currents in in lead and trail using wavelet energy entropy	55
6.1.2.2	Wavelet energy entropy analysis for Equal current with different types of electrode diameter combinations.	58
6.2	HAZ (Heat affected zone) Hardness analysis	62
6.2.1	HAZ Hardness analysis of equal and unequal current condition and different wire diameter combination.	63
6.2.2	HAZ Hardness analysis of equal current condition and different wire diameter combination.	66
6.3	Aspect ratio (P/W) analysis	68
7	Conclusion and Future work	69
7.1	Conclusion	69
7.2	Future work	69
	References	71

List of Figures

1	Twin-wire welding with single power source	3
2	Twin-wire welding with double power source	3
3	Bar chart of year-wise publication of twin-wire welding	8
4	Voltage-current cyclogram for the welding process	14
5	Methodology of work	20
6	Steps in experimental procedure	22
7	Schematic diagram of the Experimental setup	23
8	(a)-Experimental set-up of twin wire welding.	24
	(b) -Hardness testing setup	29
	(c) -Welded sample	29
	(d) - Arrangement for bead geometry measurement.	30
9	Mexican Hat Wavelet (left) and its magnitude (right).	39
10	Morlet wavelet (left) and its magnitude spectrum (right); $f_b = 1\text{Hz}$ and $f_c = 1\text{Hz}$.	39
11	Gaussian wavelet (left) and its magnitude spectrum (right).	40
12	Frequency B-spline wavelet (left) and its corresponding magnitude spectrum (right).	41
13	Shannon wavelet (left) and its corresponding magnitude spectrum (right); $f_b = 1\text{ Hz}$ and $f_c = 1\text{ Hz}$.	41
14	Procedure of a four-level signal decomposition using discrete wavelet transform.	42

15	Haar wavelet (left) and its magnitude spectrum (right).	43
16	Daubechies wavelet (left) and its magnitude spectrum (right). (a) Daubechies 2 base wavelet and (b) Daubechies 4 base wavelet.	44
17	Coiflet wavelet (left) and its magnitude spectrum (right). (a) Coiflet 2 base wavelet and (b) Coiflet 4 base wavelet.	45
18	Symlet wavelet (left) and its magnitude spectrum (right). (a) Symlet 2 base wavelet and (b) Symlet 4 base wavelet.	46
19	Electric circuit.	49
20	Energy-entropy ratio for different Basewavelet.	54
21	WEE of lead and trail current for 0.8-0.8mm wire diameter combination.	56
22	WEE of lead and trail current for 0.8-1.2mm wire diameter combination.	57
23	WEE of lead and trail current for 1.2-0.8mm wire diameter combination.	58
24	WEE for equal current of lead and trail for 0.8-0.8mm wire diameter combination.	59
25	WEE for equal current of lead and trail for 1.2-0.8mm wire diameter combination.	60
26	WEE for equal current of lead and trail for 1.2-1.2mm wire diameter combination.	60
27	WEE for equal current of lead and trail for 0.8-1.2mm wire diameter combination.	61
28	WEE v/s current density difference grap.	62
29	HAZ Hardness of dissimilar lead and trail current for 0.8-0.8mm wire diameter combination.	64
30	HAZ Hardness for 0.8-1.2mm wire diameter combination and dissimilar current.	65

31	HAZ Hardness for 1.2-0.8mm wire diameter combination and dissimilar current.	65
32	HAZ Hardness of equal current condition with 0.8-0.8mm wire diameter combination.	66
33	HAZ Hardness of equal current condition with 1.2-0.8mm wire diameter combination.	67
34	HAZ Hardness of equal current condition with 0.8-1.2mm wire diameter combination.	67
35	P/W ratio v/s current density difference graph.	68

List of tables

1	Range of current and voltage for corresponding diameter of filler wire.	2
2	Gaps and opportunities for research.	18
3	Chemical composition of the welding materials.	25
4	Mechanical property of the welding materials.	25
5	Constant parameters during the welding experiment.	25
6	Welding parameters during the welding experiment.	26
7	Specification of welding machine.	27
8	Specification of data acquisition system.	28

Chapter 1

Introduction

1.0 Overview

This chapter contains the introduction of the Twin wire Gas metal arc welding. In this chapter there are three parts. In the first part GMAW, Twin wire GMAW and their working principles have been introduced whereas the second part is introductory of the Arc stability and previous assumptions. The last section deals with the reasons of the disquisition.

1.1 GMAW and Twin wire GMAW

Welding is an ancient fabrication process which is used for the joining of material by causing coalescence. The joining can take place with or without application of heat, with or without application of pressure and with or without the use of filler material. The materials of joining may be similar or dissimilar. GMAW is one of the most widely used welding techniques due to its wide range of application in industries. During gas metal arc welding (GMAW), the arc strikes between the bare wire electrode and the work piece. The arc is shielded using the shielding gas. When the arc is shielded by the blow of inert gas then the process is known as metal inert gas (MIG) welding and if the shielding gases are the active gas like CO₂ or mixture of active and inert gases then it is known as metal active gas (MAG) welding. The electrode is connected to the positive terminal and the work piece is connected to the negative terminal in order to get the stable arc. When we connect the electrode to the negative terminal then it results into an unstable spatter arc leading to poor weld bead. The flat characteristics leads to the self-adjusting arc which leads to constant arc length. GMAW requires shielding gas and consumables as filler wire electrodes. The filler wire electrodes are 0.8, 1.0, 1.2 and 1.6 mm in diameter. In conventional welding the range of voltage and current changes with change in the diameter of the wire. The Table.1 shows the current range and the voltage range of the different mild steel electrodes.

Table 1 Range of current and voltage for corresponding diameter of filler wire [ASW].

Electrode-wire dia.(mm)	Current range(A)	Voltage range(V)
0.8	50-180	14-24
1.0	70-250	16-26
1.2	120-380	17-30
1.6	150-380	18-34

The selection of the both inert gases (argon and helium) and active gases (like carbon-dioxide and Nitrogen) for the shielding depends on the metal to be welded. For mild steel, carbon di- Oxide is normally used which gives a high quality weld. Low alloy steels are welded with the 80% argon and 20% carbon dioxide mixture.

This process is extremely versatile for a wide range of work piece thickness and for all kind of welding positions in ferrous as well as non-ferrous materials. The process is easy to mechanize and automate as continuous welding is possible and highest quality weld is produced.

The protocol to enhance the quality of weld and to increase its productivity in minimal cost has revolutionized the research in the field of welding. It has made researchers to think about the different alternatives for different kind of weldment requirement. The GMAW is a more than a five decade old process and it is still being used because of its speed to weld. But due to the demand to increase the productivity, the multi-wire GMAW welding system has become the key area of research. Twin-wire gas metal arc welding (TW-GMAW) is a kind of multi-wire GMAW process which is very much useful in increasing productivity of welding and it produces very less porosity ,less residual stress, higher aspect ratio(depth to width ratio) , lesser spatter loss and better arc stability also in contrast to the conventional single wire GMAW. In this Lead arc causes the penetration and Trail arc controls the appearance of the bead [10].The Schematic representation of the twin -wire welding has been shown in Figure 1 and Figure 2. The Figure 1 shows the schematic diagram of the twin wire welding in which both the electrodes are connected to a single power source, whereas the twin wire system having an individual power source of lead and trail has been shown in the Figure 2.

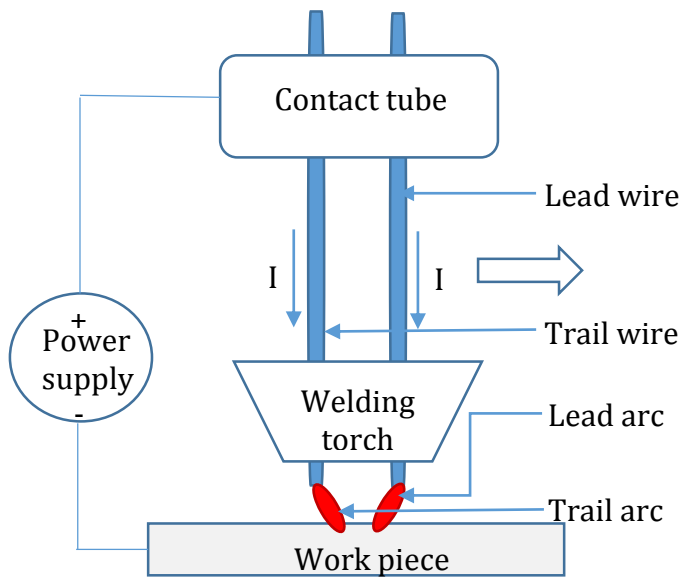


Figure 1 -Twin-wire welding with single power source.

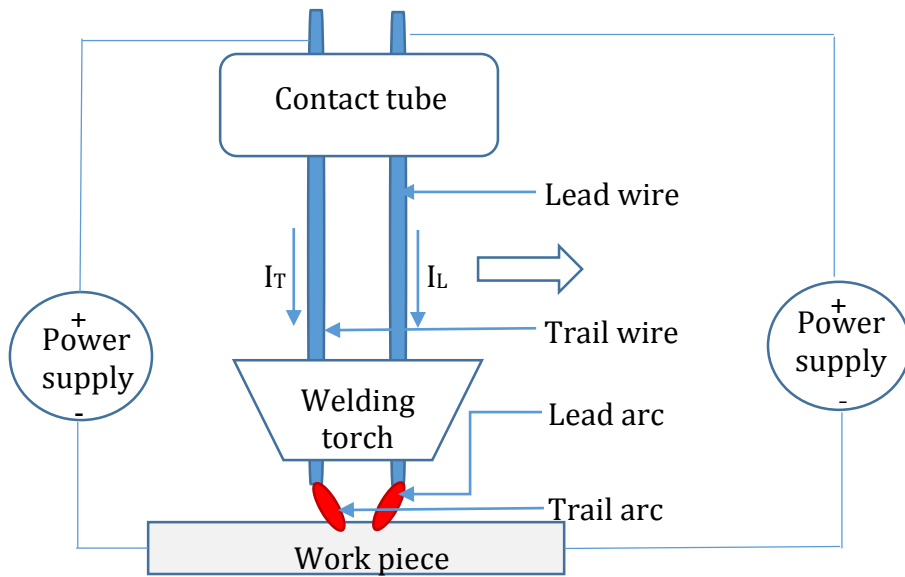


Figure 2 -Twin-wire welding with two power sources.

In a twin wire welding process if the distance between the lead and trail wire is more than the formation of two separate weld pool occurs and there is no interaction between them. So researchers suggest the name of this kind of twin wire welding as the “addition of two energies from the arc heating for same welding pass”. Whereas in another case both the arcs(lead and trail arc) have common weld pool in which the lead arc melts the base metal and the trail arc is poured into the end part of the weld pool and this process is named as TANDEM twin wire welding process[14]. During a TANDEM welding process two wires are continuously fed using a welding torch and those are consumed to form a single molten pool. These two wires are electrically isolated. There are two different wire feed system and two power sources also for the two wires. The two different wire feeders helps us in feeding wires of different diameters and we can vary the current and the power supply using individual power systems of wires.

1.2 Arc stability and previous assumptions

The quality of the weld is directly proportional to the stability of arc during the arc welding, therefore for quality monitoring of the weld, study of arc stability is important. The parameters which are considered for major effect on the Arc stability are Arc current, Arc voltage, welding speed and wire diameter. Along with all these parameters the welding torch structure also plays an important role in the Arc stability for high speed pulse TANDEM welding [1, 2]. The space and the angle between the wires and the shielding gas composition also affects the stability of arc [3, 4]. Suban et al. [4] have shown that the welding pool surface has an effect on voltage. Many researcher’s views are that the pulse current condition gives the best result in twin wire GMAW. But there is no clear explanation about the implementation of continuous current during twin wire welding. In twin wire welding if the separate power system (master and slave) for current supply in the lead and trail is provided, then we can find the stability of lead and trail arc by analyzing different current combinations like continuous-continuous, continuous-pulse, pulse-continuous and pulse-pulse. In order to check the stability of the Arc the analysis of characteristics of Arc signals is necessary. The welding arc stability makes the welding process stable. In an ideally stable arc welding process, there are uniform material transfer, constant arc length and no spatter loss. In this during short-circuit transfer the arc burning time and the short-circuiting time

should be uniform. During the pulse transfer, the material transfer should take place at the rate of one drop per pulse and for spray transfer the time between transfers of two drops should be same. The instability of Arc can be found by many methods like Acoustic emission method, High speed camera system, Electrical signal acquisition system, etc. But the least complicated process of analysis of arc stability is based on the real time arc voltage and arc current intensity [4]. The variation of current and voltage becomes very fast and this variation depends on the material of workpiece and electrode, wire feed rate, arc length, and the type of shielding gas used. The dynamic characteristic of the voltage and current is recorded as a function of time as stated below:

$$V=f_1(t) \text{ and } I=f_2(t) \quad (1)$$

Arc signals have noise due to uncertain influencing factors and those are nonlinear and vary with time. Therefore wavelet analysis of the signal is required which gives a suitable analytical result for the signal. It gives the report of a signal in a very small time period for the multi-resolution analysis. There are many wavelet functions and the selection of the best wavelet function is the first work in the path of signal analysis. By acquiring energy to Shannon entropy ratio of a given signal using different wavelet functions one can choose the wavelet function giving this maximum value is considered as the best wavelet for the analysis of the signal. Using this wavelet function WEE of all the signals can be calculated. The Wavelet analysis is described in detail in chapter 4.

1.3 Motivation

Twin-wire GMAW is being used widely in the industries due to its speed to weld and better weld properties. The arc instability is the major drawback of twin wire welding. Tandem welding is a kind of twin-wire welding. In Tandem welding process we can supply different types of currents in lead and trail wire. There are very few researchers who have shown the effect of dissimilar currents on the stability of arc and they have found that the difference between lead and trail current effects the stability of arc during the twin wire welding process. Therefore the study of the arc stability under different conditions of current becomes important. Along with all these facts there is no literature in which the effect of dissimilar wire diameter on the stability of arc has been discussed.

Few researches suggest that the stability of arc affects the hardness of the base material and the weld bead geometry. Since HAZ zone is the critical zone in the welded material therefore it can be helpful in the analysis of arc stability.

In very few literatures the arc stability been analyzed using wavelets. It has been found that by using wavelets we can quantify the stability of arc in a much better way than the other arc stability analysis methods like Cyclogram, PDD, Fourier transform etc. By using wavelets we can analyze the stability of arc at a certain time period and the uncertainty in the arc stability can be visualized.

Chapter 2

Literature review

2.0 Overview:

The literature review is basically categorized into four parts. The first part deals with the birth and evolution of twin wire welding. The second part deals with the review on twin wire welding. The third part deals with the review on arc stability. The fourth part deals with the opportunities in the present scenario. The latter portion is dedicated to the formulation of the present work.

2.1 Birth and evolution of twin wire welding:

Due to the industrial revolution there was a great demand was to increase the productivity and quality with reduction in the cost of production. The maximum impact of it was upon the manufacturing sector. Since the welding is the one of the best material joining process in the manufacturing therefore the need of multi-wire welding system came into the picture. Using the multi wire welding system one can do welding in a fast manner when compared with traditional single wire welding system. The first time twin wire welding system was implemented in submerged arc welding by Asthon [5]. Later the implementation of the twin wire welding have been done for GMAW, GTAW, laser welding etc. But it has been found that the weld quality of the GMAW is better than the weld produced through SAW process for e.g. the residual stress generation happens more in SAW process than GMAW process[6]. The GMAW is a five decade old process but the twin wire GMAW was first introduced in 1989 by Lassaline [7]. Later this technique became one of the most useful welding techniques and researchers are still working to enhance this technique. The Figure 3 depicts the bar chart of the published articles of twin wire GMAW in the last one and half decade (Source-Scopus) and from the bar chart, it is quite clear that the researchers have deeper interest in the twin wire GMAW process.

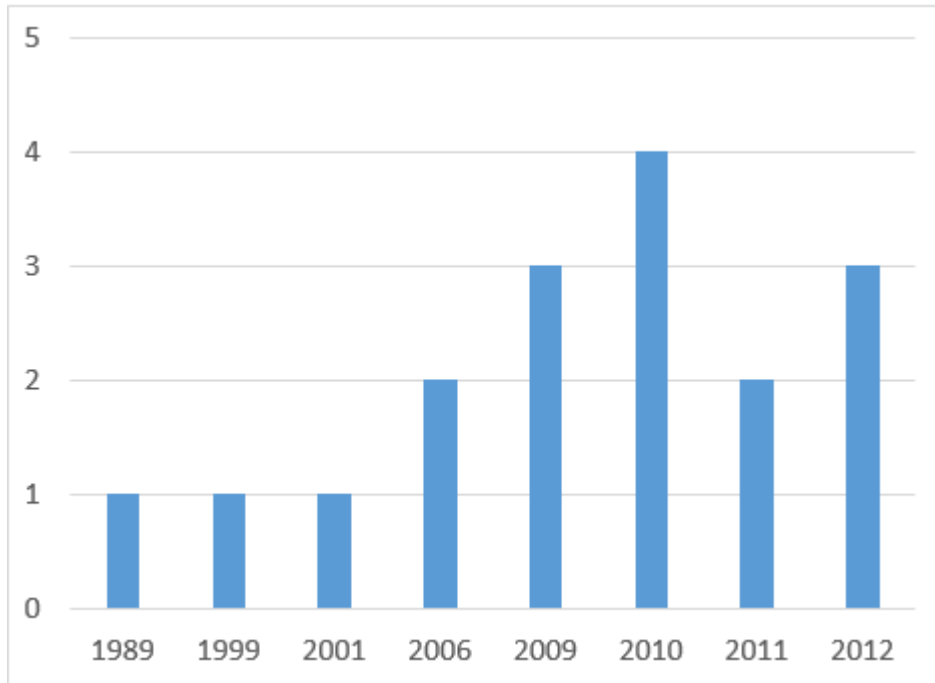


Figure 3 -Bar chart of year-wise publication of twin-wire welding.

2.2 Review on twin wire welding

UEYAMA et al. [1] has described the electromagnetic interference between lead and trail arc in twin wire submersed arc welding and they have given the preventive for it. It is described that the pulse timing control between the lead and trail wire is necessary to prevent the arc extinguishing. It has been suggested that the pulse peak current of the trail wire should be delayed by 0.5ms that for the lead wire to reduce the interference. In this paper the effect of the inclination angle of the electrode wires, distance between the wires and the ratio of the trail and lead current on the arc interference and weld properties have been studied. In the study it is found that if the speed of welding is 3m/min and push angle of the trail wire is 9-degree regardless of lead wire inclination angle then the sound weld bead with uniform thickness can be achieved. The 9 to 12mm distance between the lead and trail wire is useful to maintain the maximum speed of welding. The proper range of trail and lead current ratio has been suggested as $I_t/I_L = 0.31$ to 0.5. Using all these given values of parameters the

maximum welding speed has been achieved for 4 to 4.5 m/s which is about three times higher than the single wire pulse GMAW.

Tuslek et al. [8] have done the mathematical modeling for the melting rate in twin wire submerged arc welding. The comparison between the practical value of the melting rate of metal and the value after doing the mathematical modeling has been done. It has been found that it is more accurate than the prior mathematical modeling processes. In this it has been shown that the melting rate of material in twin wire system is more than twice the single wire system. Along with this it has been shown that for the same value of parameters of welding the melting rate of the thinner wire is more than the thicker wire.

Sharma et al. [9] have done the mathematical modeling for the flux consumption during twin wire welding. It has been found that for DCEP there is no any effect of the speed and CTWD on the consumption of the flux. Whereas when there is DCEN these factors affect the consumption of the flux.

Sharma et al. [10] have investigated the behavior of arc in twin wire submerged arc welding. The behavior of the arc have been studied with the help of transient heat transfer analysis and it has been found that the leading arc causes the penetration and the trail arc causes the heat generation.

Kiran et al. [11] have shown the arc behavior in twin wire submersed arc welding. They studied the root dimension of leading arc and trailing arc and the arc interaction. The real time current and voltage waveforms were recorded and the CCD arc images were taken for a wide range of the experimental condition. The influence of arc interaction on the molten metal transfer was studied. It was found that the arc root dimensions were unsymmetrical and were increasing with increase in current and voltage and decreasing with increase in arc center displacements. It has been shown that trailing arc center displacement is more sensitive than the lead arc and for a constant lead current the decrement in the trail current makes the latter more unstable.

Ma & Zhang [12] have introduced the noble double electrode gas metal arc welding process for the welding of steel tube in simplified conditions. In this paper it has been shown that the

main arc current and bypass current are the key factors in producing a good quality welding seam. The arc pressure can also help in reducing flatter quantity and to improve weld quality. The distance between the torch and the work piece has also a great impact on the welding quality. The angle between the torches have a higher impact on the arc ignition and the flatter. It has been found that the 30° angles between lead and trail is suitable for high quality weld.

Wei et al. [13] has worked on consumption of double electrode in single arc. In this it has been declared that the distance between the main wire and bypass wire decides whether the welding process could be successful or not. If the distance between them is too small then there will be interference between them where as if the distance is too big then the bypass wire will not melt. Therefore the optimal distance should be maintained.

Fan and Lu [14] have worked on consumable DE-GMAW. They have developed a fuzzy control system by using which good weld bead and stable welding process can be obtained.

Wang and Zhang [15] have developed image processing algorithm for the automated monitoring of the metal transfer in double-electrode GMAW. Since the transfer of the molten metal is very much important for the quality of the weld. In this article a brightness based system has been located to compute the droplet automatically.

Li and Zhang [16] have observed that in double-electrode GMAW the critical current of the spray transfer can be lowered, the droplet trajectory can be shifted, the diameter of the droplet can be reduced and the speed and rate of droplets can be increased when compared to the single electrode GMAW system.

Li and Zhang [17] have done modeling and control of consumable Double-electrode gas metal arc welding. In this article it is found that the state of bypass arc voltage can be used to predict and monitor the stability of the welding. The uncertainty of the process can be easily described by the model developed.

Wu et al. [18] have shown that during double-electrode twin wire welding if the welding speed is increased beyond a certain speed then the humping bead formation will occur. When the welding speed was up to 1.7m/min, then no any humping occurred.

Stephen et al. [19] have studied and evaluated the surface residual stress in the double electrode butt welded steel plate. It has been found that the final stresses for the double electrode case remains higher than the single electrode case for longitudinal and transverse load. In this the observation has been done for the concentration of the residual stress also. It has been found that for the double electrode case the distribution of the maximum residual stress is in the HAZ and in the base metal closer to the filler metal. Whereas in the single wire case it has been found that maximum stress value were located along the deposited metal.

Meng et al. [20] have analyzed the temperature field and the stress field in the twin wire welding of Al-alloy. In this it has been found that the lead arc and trail arc form the double ellipsoid after the deflection. Based on this the amendment of heat source model has been done. After doing the comparative study of single wire welding and twin wire welding it has been found that the heat affected zone (HAZ) is narrower in the twin wire welding when compared with single wire welding. Therefore the twin wire welding is helpful in reducing the hot crack generation and the over-aging softening defect.

MOTTA et al. [21] have investigated the effects of variables on the weld bead geometry during the twin wire MIG/Mag process. In this the convexity index, mean penetration in sides, penetration in the center, the profile of penetration and the portion of the diluted area has been measured for different experiments. The different stages of results have been shown in which the first stage shows the effect of the lead and trail wire angle on the weld bead geometry. The second stage of it shows the effect of the mean current, phase displacement, electrode positioning and the arc length effects on the weld bead shape. After the analysis it has been found that the penetration becomes narrow and deeper when the tandem electrode is used instead of side by side and the similar kind of tendency is observed when the in-phase pulses are used instead of out-of-phase pulses. Another observation shows that larger the angle between the electrodes provides the better dilution and penetration. The suggestion given for the application of twin-wire welding is that one should use the low mean current for lead and trail arc, side-by-side lead-trail position and out-of-phase pulses of current. If someone wants to do weld in joints, then the mean current of electrodes should be increased to a higher value and the pulses of current should be in-phase. These kind of welding is preferable in chamfered joints.

The better conclusion of this paper is that

(a) More the angle between the electrodes provides an extra deep and the more uniform penetration and it also increases the dilution.

(b) Increment in the arc length causes the beads with reduced penetration and smaller width.

(c) Increasing the mean current leads to increase in the weld bead width, depth of penetration, dilution and the flatness.

(d) If the position of the electrode is changed from side-by side to tandem then the depth of the penetration increases at the center and the uniformity in penetration increases.

Han et al. [22] has studied the arc phenomenon and fusion of core wire in twin wire single arc welding (TESAW). In this arc voltage and current are measured by oscilloscope. It has been found that the arc in TESAW fluctuates periodically after a time period of 20-40ms and corresponding to this the arc voltage also changes periodically. But there is no variation in arc current. There is not any short-circuiting phenomenon found during the combustion process of arc. The formation, growth and detachment of droplets change the arc shape and effects the arc voltage fluctuation. Welding current, type of electrode and two core span are the prime factors for the core wire fusion and arc voltage fluctuation.

Dingjian et.al [23] has shown that during twin wire welding the arc interaction increases the droplet transfer frequency. Along with that the droplet size decreases and at the same time wire length also decreases.

Cho et al. [24] have studied the behavior of the molten pool during tandem submerged arc welding. It has been developed a three dimensional model of heat transfer and fluid flow to examine the temperature profile, velocity field, weld pool shape and size. This model solves the conservation of mass, momentum and energy. Afterwards a scheme to handle the arc interaction has been introduced. Using the computational fluid dynamics it has been found that the droplet transfer and the arc of the leading electrode heavily effects the molten metal pool pattern.

2.3 Reviews on arc stability:

Among the welding processes the arc welding is most widely used. Due to implementation of automation in industries there is a need of real-time monitoring and control of welding. In a Gas metal arc welding process we can get the larger penetration, higher welding speed and high deposition rate. It is suitable for curved, straight, long and short joints through welding. It is suitable for both thin sheets and thick sheets. But the spatter loss is one of the main drawbacks in GMAW. When we take a gas mixture (80%Ar + 20%CO₂) for shielding of arc then the spatter loss decreases and the bead appearance becomes better but the quality of weld depends more on the stability of arc. The behavior of arc in twin wire welding is our prime concern of study. The arc instability causes arc spatter which leads to loss of material and reduces productivity. This also need cleaning process and gives unaesthetic appearance. Many methods of arc stability have been given in the literature like study of arc light, study of sound emitted, noise analysis etc. Suban and Tusek [4] have defined several method to study the arc stability in GMAW like voltage-current cyclogram, Probability density distribution (PDD) of current and voltage, burning and short circuiting time of arc, probability distribution of the short-circuiting. According to them there are numerous parameters which affect the stability of arc. They studied the effect of different shielding gases on the stability of arc. They have done analysis of welding process stability base on welding current intensity and the welding voltage. According to them a process of welding is stable if such conditions have been obtain:

- (a) The material transfer should be uniform.
- (b) The arc burning time and the short circuiting time should be uniform along with the short circuiting period.
- (c) During spray transfer the time period between the transfers of two drops should be same.
- (d) During pulse transfer one drop per pulse should take place.
- (e) The arc length should be constant.
- (f) There should not be any spatter loss.

The least complicated method to analyze the stability during the welding is based upon the welding current intensity and voltage where the statistical analysis of the voltage and current signal is done. They carried out the experiment on the low alloy structural steel and for that the selected filler material was a solid wire of diameter 1.6mm of quality SG2. They used three types of shielding atmosphere, pure CO₂, a two-component 82% Ar/18% CO₂ gas mixture, and a four-component transferred ionized molten energy (TIME) gas mixture (65% Ar/26.5% He/8% CO₂/ 0.5% O₂). The measurement system consisted of a shunt, low-pass filters, analogue-to-digital and digital-to-analogue (A/D-D/A) converters, and a personal computer. The sampling frequency of the measurement chain was 6 kHz.

During the welding the current and the voltage vary due to the variation in the arc length. That's why these are called dynamic characteristics. cyclogram has been introduced to check the stability of the arc which has been shown in the Figure 4.

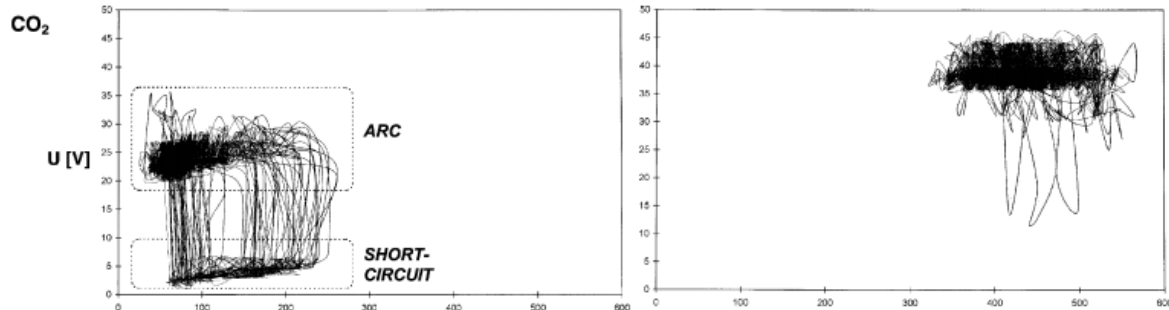


Figure 4- Voltage-current cyclogram for the welding process [31].

In the Figure 4, the short circuiting zone has been introduced in the cyclogram and when the short circuiting is more the spatter loss is more and the arc will be less stable.

Li et al. [24] has used the wavelet energy entropy for the analysis of the arc stability of square wave alternating current of submersed arc welding. In this article the multi resolution analysis have been combined with the Shannon information entropy. The wavelet

energy entropy have been applied to analyze the current signal in square wave alternating current submerged arc welding. In this article it has been shown in this article that the more stable a welding process is lesser is the value of information entropy.

Moinuddin and Sharma [25] has conveyed one new observation for the arc stability in the twin wire GMAW which is anti-phase synchronized and synergic pulsed. The information about three modes of PDD has been given in this paper. Mode.1 of the PDD indicates the probability of the dip transfer, Mode2 indicates the probability of the globular transform and the Mode3 gives the probability of the spray transfer.

In this paper it has been shown that the dissimilar currents at lead and trail are able to stabilize the arc. The effect of arc stability on the weld bead geometry, hardness, heat affected zone and hardness of weld have been shown. This paper suggests that the lead and trail current should be dissimilar to reduce the arc interaction. Equal currents at lead and trail causes the maximum dip transfer and least spray transfer whereas the higher current at lead electrode increases the probability of spray transfer in both electrodes. In the unstable arc case, it is found that the hardness increases linearly from weld center to HAZ. The penetration-width ratio and melting efficiency increases with the higher value of lead current which is reflected by narrower HAZ.

Azar et al. [26] have done the statistical analysis for the behavior of arc in the dry hyperbaric GMAW. It has been found that at higher pressure the voltage and current have great influence on the stability of process .At low pressure the voltage and current waveforms have the same kind of waveform but for hyperbaric case the waveform of voltage changes from the waveform of current. But the power is constant when there is no correlation between current and voltage waveform. In this it was observed that the frequency of the voltage and current waveform were lower in hyperbaric case. A Fourier analysis has been done for the analysis of mass transfer change with the increase in ambient pressure. The observation shows that the base current generation is more frequent than the peak current generation. The calculated arc power shows that more energy is required for arcing at higher pressure.

Luksa et.al [27] have investigated the effect of weld imperfection on the stability of arc. The work is focused upon the quality control of the GMAW process therefore the method for

quick and safe data analysis is required. For the quick analysis the momentary arc resistance and the momentary arc power has been analyzed. The output has been compared with the output of the current and the voltage signal of the arc .The artificial disturbance has been created and correspondingly the mean value of sensitivity and the variance of signal has been analyzed. It has been shown that from the analysis it is possible to detect the imperfection also. The disturbances produced artificially are lack of shielding gas, a layer of grease on the plate, layer of paint, too narrow root gap and too wide root gap .The Nitrogen, Oxygen and Hydrogen are formed due to decomposition of grease and paint. These gases change the shielding property, the surface tension in the pool of molten metal, the ionization potential, the arc ignition condition, the welding arc power and many other factors in arc burning. Lack of shielding gas also affects the shielding of arc. All the kind of disturbances change the arc burning condition.

There are few paper on welding in which the possibilities of enhancement of the process has been discussed .Those papers are:

Suban et al. [31] has described that the use of the shielding gas effects the melting rate in MIG/MAG welding process. There are different types of shielding gases have been used in which the number of components varies from one to four. The criteria for the selection of the shielding gas depends on the quality of weld produced using it. The analysis has been done for the cored wire, solid wire and covered wire electrode melting rate characteristics also. Later the electric and thermal conductivity of the gases have been analyzed and their effect on melting rate have been studied. After that the analysis has been done for the melting rate as a function of current for different conditions and these conclusions have been found that

(a)In the same parametric condition the cored wire melting rate is higher than that of solid wire.

(b)Shielding gas medium has no any effect on the melting rate for the same parametric condition of welding.

Murphy et al. [32] has found two major effects of metal vapors on the plasma of arc in GMAW: (a) decrease in temperature in the whole arc region and (b) Formation of localized

minimum temperature near the arc center. For the first effect the reason is found that the increment in radiative emission and influx of metal vapor. The second effect is also a consequence of the in fluxing of metal vapor in the flow.

Pal et al. [33] has investigate the metal transfer with the arc sound in pulsed GMAW and it is found that the arc is strongly related to the parameters of process and the weld quality.

Valter et al. [34] has shown that the stability in metal transfer during welding leads to lesser generation of fumes. The study of the great transfer stability indicates that it doesn't affect the fume generation but it reduces the spatter loss. The conclusion is that the fume generation and spatter generation has no correlation. The increment in the fume generation is due to the higher short-circuiting current, large droplet diameter before detachment, longer arc length, longer arcing time and many more factors.

There are some papers which have been referred for the wavelet analysis. The wavelet analysis has been discussed in detail chapter4.

2.4 Gaps and opportunities:

From the literature review it has been found that there are lots of gaps and opportunities. Those gaps and opportunities are discussed in the Table 2.

Table 2 Gaps and opportunities.

Sl.no.	Gaps	Opportunities
1	There are very few literature on arc stability of twin-welding and very few people have worked on the dissimilar currents in lead and trail.	The effect of similar currents and dissimilar currents on the arc stability can be compared.
2	There is no literature on the arc stability of dissimilar wire combinations in lead and trail.	The effect of different combinations of wires of different diameters on the arc stability can be studied.
3	Wavelet analysis of twin-wire welding has been done in very few literatures.	The signal analysis using wavelet transform can be helpful in monitoring and enhancing the welding process.
4	The effect of variation of current density has not been discussed in any literature.	The effect of current density on arc stability can be studied.

Chapter 3

Objective and methodology

3.0 Overview

This chapter contains three parts. In the first part problem statement has been given. In the second part objective of the work have been produced. In the last section the diagram of the methodology has been given.

3.1 Problem statement:

"Arc stability analysis of twin-wire welding using wavelet energy entropy."

3.2 Objective:

1. To study the effect of the types of current combination in the lead and trail on the stability of lead and trail arc.
2. To study the effect of dissimilar wire diameter on the stability of arc in Twin-wire GMAW.
3. To study the effect of increase in current for the same current value in the lead and trail in twin-wire GMAW.
4. To do a comparative study to find the optimum parameters for the arc stability.

3.3 Methodology

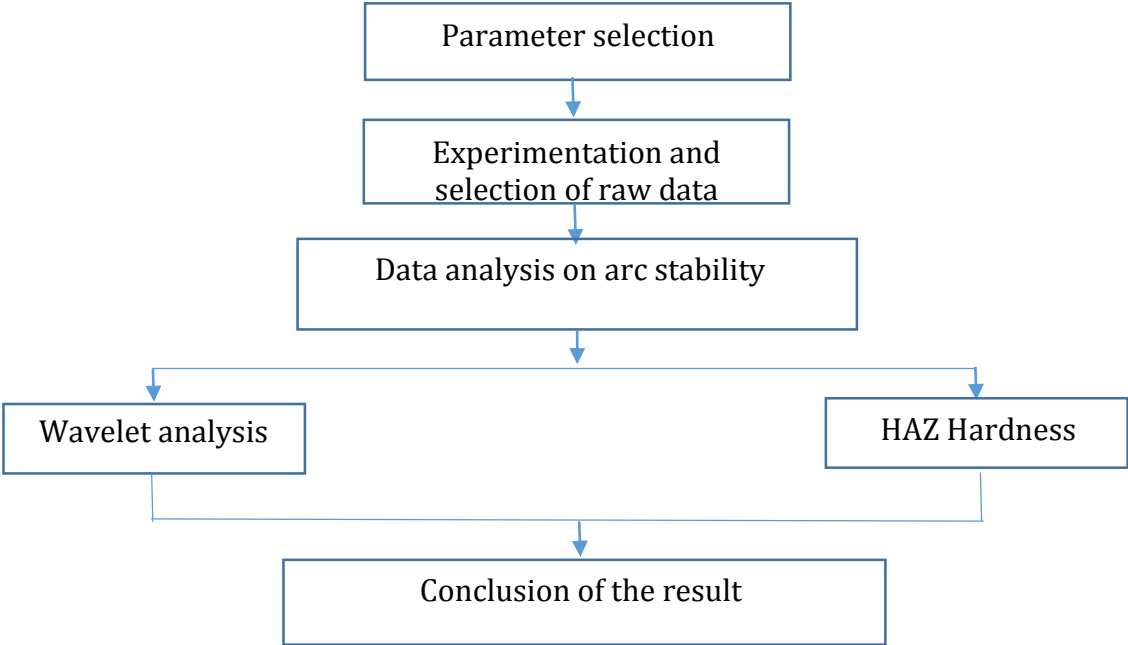


Figure 5 -Methodology of work.

Chapter 4

Experimental procedure

4.0 Overview

The design of experiment has been done based on the allowable range of the welding parameters. It has been performed different set of experiments which can be basically categorized into two groups. In the first group the experiment has been conducted for the Equal currents in lead and trail with different types of electrode diameter combinations. In the second group the experiments have been performed for the Unequal currents with different types of electrode diameter combinations. The schematic diagram of Experimental set up given in the Figure 7 and the experimental setup has been shown in Figure 8(a).The experimental procedure has been divided into four steps. In the first step the selection of the material and process parameter has been done which has been discussed in the first section. The second step is the twin -wire welding process and this has been discussed in the second section of this chapter. The third step is data acquisition which has been introduced in the third section. The last step is HAZ Hardness and bead geometry measurement which has been discussed in the last section. The different steps of experiment have been given below.

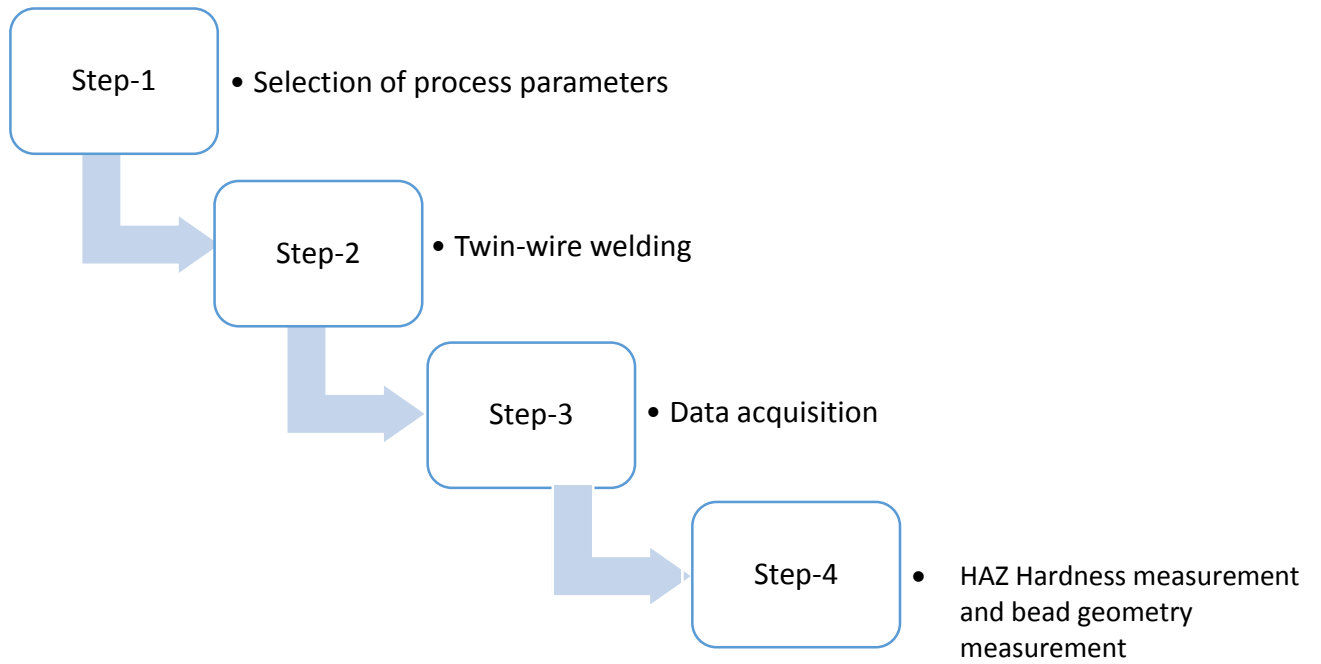


Figure 6-Steps in experimental procedure

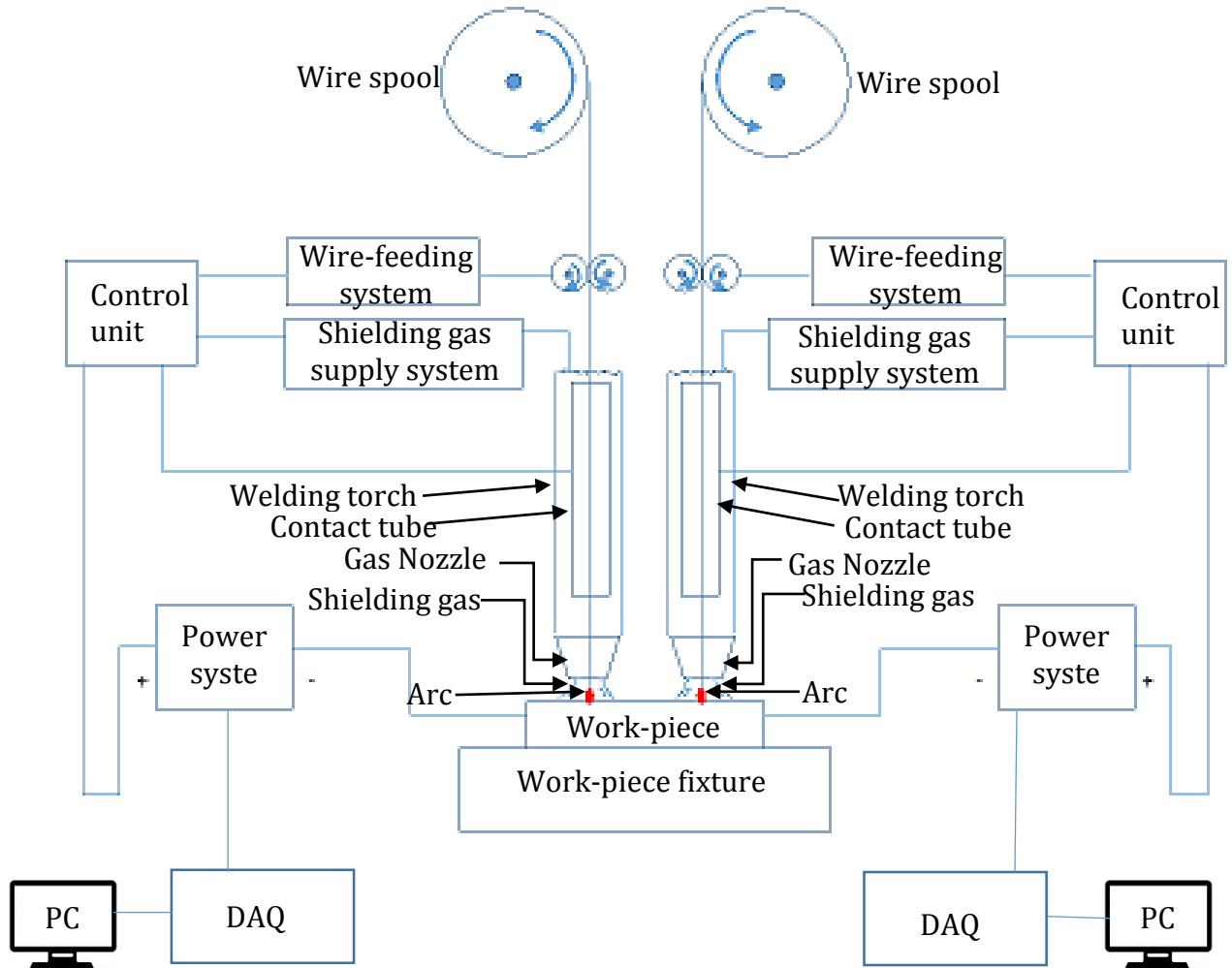


Figure 7-Schematic diagram of the Experimental setup for twin wire welding.



Figure 8(a)-Experimental set-up of twin wire welding.

4.1 Selection of material and process parameters:

This particular section deals with the selection of the material and the process parameter. This section has been divided into two sub-sections. The first section deals with the selection of material and the last section deals with the selection of process parameter selection.

4.1.1 Selection of material:

The base metal used for the welding experiment is Mild Steel IS 2062-2011 (Grade A mild steel). The dimension of the base metal is 300x 75 x 10 mm. ER70S-6 (AWS A5.18) was selected as filler material. The chemical composition and the mechanical property of the base material and filler material have been given in the Table2 and Table3 correspondingly.

Table 3 Chemical composition of the welding materials.

Elements	C	Si	Mn	P	S	CE	Fe
Base material	0.211	0.206	0.71	0.015	0.018	0.351	Balance
Filler material	0.07- 0.15	0.80- 1.15	1.85 max	0.025max	0.035max	-	Balance

Table 4 Mechanical property of the welding materials.

Mechanical property	Yield strength(psi)	Tensile strength(psi)	Elongation percentage in 2"
Base material	49-87000	62-11lakh	23%
Filler material	70-75000	85-90000	28%

4.1.2 Process parameters:

The selection of the parameter is very much important to control the arc instability, spatter loss and fume generation. Welding current, welding voltage, CTWD and welding speed are commonly used parameters for the arc welding. From the literature, it is found that the angle between the lead and trail wire, the gap between leadership and trail arc, ratio of lead and trail current and type of shielding gas also affect the arc welding. Few parameters of the welding had been kept constant throughout the experimental process which are given in the Table 4.

Table 5 Constant parameters during the welding experiment.

Welding parameter	Value
CTWD	20mm
Gap between lead and trail	5-7mm
Angle between lead and trail	7°
Gas flow rate	15lpm

During the welding process the power supply is always in synergic mode. In synergic mode power supply if we feed only one welding parameter, then it is enough for the welding process. Because all other parameters like (welding voltage and welding speed) are automatically controlled by the system.

Table 6 Welding parameters during the welding experiment.

Equal current with different types of electrode diameter combinations.				
Sl.No.	I _L (A)	I _T (A)	Current combination	Electrode dia. Combinations
1	140	140	Pulse-Pulse	Ø0.8-Ø0.8, Ø1.2- Ø1.2, Ø0.8- Ø1.2 and Ø1.2- Ø0.8
2	160	160		
3	180	180		
4	200	200		
Unequal current with different types of electrode diameter combinations.				
5	180	140	Pulse-Pulse	Ø0.8-Ø0.8, Ø0.8- Ø1.2 and Ø1.2- Ø0.8
6	180	160		
7	180	180		
8	180	200		
9	180	220		
10	200	180		
11	220	180		
12	220	240	Pulse-Pulse	Ø0.8- Ø1.2
13	220	260		
14	220	320		
15	240	220	Pulse-Pulse	Ø1.2- Ø0.8
16	260	220		
17	280	220		

The process parameter has been established for the two types of conditions of current combinations. In the first condition the lead and trail current has been kept equal for the first four cases (1-4) of the experimental conditions given in the Table 6. These experiments have been performed for the four different types of electrode diameter combinations ($\emptyset 0.8$ - $\emptyset 0.8$, $\emptyset 1.2$ - $\emptyset 1.2$, $\emptyset 0.8$ - $\emptyset 1.2$, and $\emptyset 1.2$ - $\emptyset 0.8$). In the second condition Unequal current with different types of electrode diameter combinations have been taken. These experiments have been given in the Table 6. The first seven experiments (5-11) have been conducted for the three different types of wire diameter combinations ($\emptyset 0.8$ - $\emptyset 0.8$, $\emptyset 0.8$ - $\emptyset 1.2$, and $\emptyset 1.2$ - $\emptyset 0.8$), the experiments (12-14) have been conducted for the ($\emptyset 0.8$ - $\emptyset 1.2$) wire diameter combination and the last three cases (15-17) have been performed for the ($\emptyset 1.2$ - $\emptyset 0.8$) wire diameter combination.

4.2 Welding of the work-piece:

For welding, the specimen material was taken a Mild Steel IS 2062-2011 (Grade A mild steel) with a 10-mm thickness and that was cut into dimensions of 75 x 300 mm². The Equipment used for welding are Fronius welding machine, Six axis Robotic (Kuka made), Shielding gas supply containing a mixture of 82% Argon and 18% CO₂. In the twin wire welding there are two separate power systems, Master and Slave. The master supplies power to the lead and slave to the trail. The synergic pulse mode of the power supply had been selected for throughout the experimental work. The gas flow rate is kept constant (16lpm) throughout the experiment. The contact tip to work-piece distance was 20mm and Electrode wire diameter was 1.2mm for each case of welding. The specification of the welding machine has been given in the Table 7.

Table 7 Welding machine specification.

	Current range	Voltage range	Welding speed
Fronius welding-machine	0-500A	0-40V	0-5m/min

4.3 Data Acquisition:

Data Acquisition system was used to record the real time signal data of current and voltage. This system consists sensor devices to sense real time current and voltage and the two separate computers with installed Arc-client 3000p software. From the data acquisition system we can obtain the data of current and voltage signal for lead and trail separately. During the experiment the data of the current and voltage signal has been acquired at the rate of 5000 data per second. The specification of the Data acquisition system has been given in the Table.

Table 8 Specification of data acquisition system.

	Current range	Voltage range	Sampling rate
Arc-agent 3000P	+/-1000 A	+/- 100 V	13,510 kHz

4.4 HAZ Hardness and weld bead geometry measurement:

Hardness is the resistance to indentation. It is the property which gives resistance to permanent deformation. Higher the hardness value indicates the high resistance for indentation. Hardness of a material depends on its toughness, elastic and plastic properties.

Figure 8(b) represents the hardness testing setup. There are three different sizes of indenter. The machine is connected to computer by the software called IMS. Base is to hold the work piece in proper position. With the help of IMS software, it is possible to give constant feed to the base. So that at equal interval of distance equal indentation is made.

Figure 8(c) shows one of the welded sample and sample 8(d) depicts the arrangement for bead geometry measurement. Data plot digitizer software was used to measure the geometry of the weld bead. The depth of penetration and the width of the weld was measured. The scale used in the figure is quite helpful in scaling of the axes of the plot.



Figure 8(b) –Hardness testing setup.



Figure 8(c) –Welded sample.

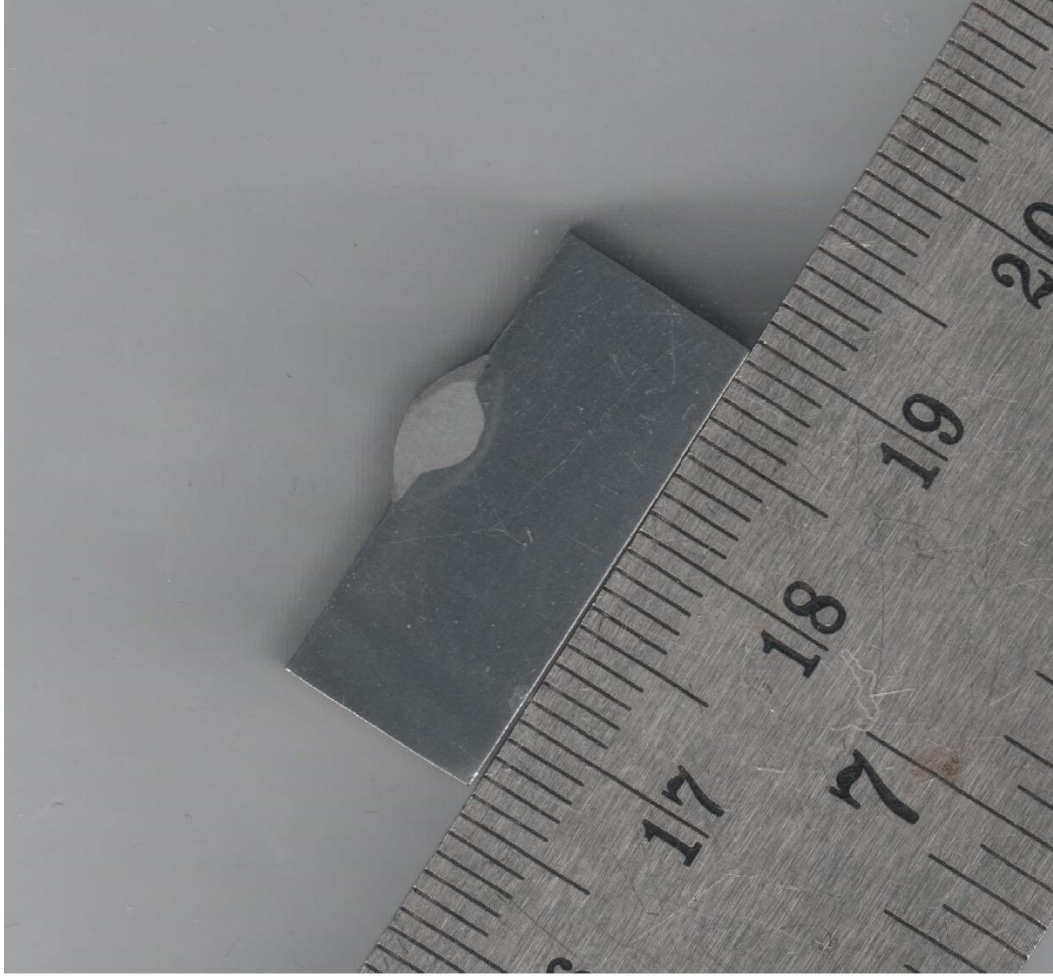


Figure 8(d) – Arrangement for bead geometry measurement.

Chapter 5

Wavelet transform

5.0 overview

This chapter consists of nine parts. In the first part the wavelet transform has been introduced. The second subsection deals with the roles of signal of signal processing. The third subsection deals with the historical prospective of the wavelet transform. The fourth subsection deals with the transform of the signal. The fifth subsection deals with the selection of base wavelet. The sixth section deals with the Entropy of the signal. The seventh subsection deals with the Energy of the signal. The eighth subsection deals with the wavelet energy-entropy. The last section deals with the Criteria for the wavelet selection.

5.1 Introduction of Wavelet transform

The transformation of a signal is done to get the information which we can't get directly from the signal. The transformation of the signal can be done in different ways like Fourier transform, Wavelet transform, etc. The Fourier transform is the most famous signal transfer technique. The spectral content of the signal can be extracted using the Fourier transformation but we can't find the spectral component in a particular time, that's why it is not a suitable technique for non-stationary signal where we don't have to find the frequency content of signal only. For example if we are analyzing the ECG (Electrocardiography) signal for diagnosis then the uneven patterns in the signal can't be analyzed using the Fourier

transform but in this case wavelet analysis and Short term Fourier transform(STFT) is very much suitable because they give Time-Frequency representation. In order to get the better resolution Wavelet transform is used more when compared with the STFT.

According to Heisenberg uncertainty principle “Momentum and the position of a moving particle can’t be found simultaneously” and this applies in signal analysis as that the frequency and time information of a signal can’t be found at a given point of time i.e. we can’t know that what is the spectral component of a signal in a given point of time.

In the wavelet transform the higher frequencies can be easily resolved in time and the lower frequencies in frequency. Therefore we can do the investigation of the spectral component in a given time interval. Here the fixed resolution is provided by the STFT whereas we can get variable resolution using the wavelet transform that’s why Wavelet is more preferable over the STFT.

5.2 Roles of signal processing in welding:

There is a significant role of the signal processing in welding. It can be used to produce a high quality weldment with low welding cost, to enhance welding equipment, to control the process of welding and for the monitoring of the process signals [35-38]. It can be used to obtain the real time information for the following purposes:

1. To identify the welding faults at the emerging stage such that we could take the corrective measures before the significant welding work would have been done.
2. To accurately control the quality of weld which is directly related to the welding conditions.

Signals (voltage and current) encountered during welding contains mainly three components:

1. A periodic component which is due to the cyclic processes happening in the welding which can be seen in cyclogram.

2. A transient component which is due to the rarely occurring events like uneven flow of shielding gas, due to improper cleaning of nozzle and due to spatters.

3. Noise in the signal.

These existing features in the signal provide us the real time information of our interest. Because of the small amplitudes and short duration of the signal, the extraction of these information is the main difficulty in the process of the signal analysis. Sometimes these signals get buried under the strong background noise which also makes detection difficult [39-41]. Along with these problems the transient nature of the signal also makes the detection difficult and the assumption of stationary signal becomes invalid. Due to this the conventional processes of Signal processing like Fourier transform becomes invalid or inefficient for these kind of signals. In past few years the Time-Frequency and time-scale techniques have been used the signal processing of the non-stationary signals. Among these processes of signal processing the Short-time Fourier transform (STFT) and Wavelet transforms are the typical representatives. Short-time Fourier transform is the extension of the Fourier transform and it addresses the inherent limitations of the Fourier transform. The Fourier transform basis function extends over an infinite period that's why it is not suitable for the non-stationary transient signal where as in the STFT the Fourier transform is performed in a localized time period. The window function chosen may be Hamming, The Hann or the Gaussian function. When Gaussian function is chosen as the window function then the STFT is called the Gabor transform [43]. The biggest drawback of using STFT is time resolution where the little separation in the time of two signals can be discriminated and on the other hand the bandwidth can't be chosen simultaneously according to the rule principle of uncertainty [44]. The product of the time and the bandwidth of the STFT must be more than or equal to the 4π . If the window function is Gaussian function then the product will be equal to the 4π .

To overcome the limitations of resolution in the Gabor transform the wavelet transform have been started to use for non-stationary signals. In wavelet transform we use short windows at high frequency and long window at low frequency. In Fourier transform the signal is expressed as a sum of sine and cosine functions where as in wavelet transform the signal is decomposed into a set of basis function. These basis functions are obtained from

two-step operation of a single base wavelet function which are (a) scaling and (b) time-shift. Scaling is done by contraction and dilation of the wave function along the axis of time whereas Time-shift is the translation through the time axis. The wavelet transform finds the similarity between the base wavelet and the signal being analyzed. Thus the conclusion comes that the wavelet transform is a powerful mathematical tool for the non-stationary signals and by using this we can do analysis, characterization and the classification of the non-stationary signals.

Since the wavelet transform has the adaptive and multi-resolution capability that's why it is suitable for the decomposition of the signals of varying time and frequency.

5.3 A Historical prospective of the wavelet transform:

5.3.1. Fourier transform: The Fourier transform is the most widely used signal processing tool. It gives the information about the frequency composition of a time series $x(t)$ when it is transformed from the time domain to frequency domain. According to Fourier 'any aperiodic signal can be represented by a weighted integral of a series of sine and cosine functions. Thus the Fourier transform of a signal $x(t)$ can be stated as:

$$X(f) = \langle x, e^{i2\pi ft} \rangle = \int_{-\infty}^{\infty} x(t) e^{-i2\pi ft} dt \quad (2)$$

By assuming that the signal has finite energy,

$$\int_{-\infty}^{\infty} |x(t)|^2 dt < \infty \quad (3)$$

And the inverse Fourier transform of the signal $x(t)$ can be expressed accordingly as:

$$x(t) = \int_{-\infty}^{\infty} X(f) e^{i2\pi ft} df \quad (4)$$

Since the signals obtained in the experiment are through Data acquisition system (DAQ) in which data obtained is discrete in nature that's why such types of signals can be transformed using the discrete Fourier transform (DFT), defined as:

$$DFT(f_n) = \frac{1}{N} \sum_{k=0}^{N-1} x_k e^{-i2\pi f_n k \Delta T} \quad (5)$$

Where ΔT is the discrete time interval, T is the total time of measurement, N is total number of samples where

$N = T/\Delta T$. The term f_n indicates the discrete frequency component where $f_n = n/T$, $n=0,1,2,3,\dots,N-1$ are the discrete frequency component.

The inverse discrete Fourier transform can be expressed as:

$$x_k = \frac{1}{\Delta T} \sum_{f_n=0}^{(N-1)/T} \text{DFT}(f_n) e^{i2\pi f_n k \Delta T} \quad (6)$$

The equation 2 and 4 shows that the Fourier transform is a convolution between time series ($x(t)$ or x_k) and sine and cosine functions.

5.3.2 Short-time Fourier transform:

Since the Fourier transform is the measure of the content of the frequency in the signal but it doesn't give the time frequency relation. Therefore to overcome the drawbacks of Fourier transform a time-localized Fourier transform was performed which is called Short-time Fourier transform (STFT). In STFT a sliding window function $g(t)$ is employed which is centered at time τ . The Fourier transform (for localized time) is performed for each specific τ then window moves along the time-line by τ and another time-localized Fourier transform is performed [42]. By performing such operations in a consecutive manner the transformation of entire signal can be performed. Hence, unlike the Fourier transform the STFT gives a 2D time-frequency representation after the decompositions.

By using the notation of the inner product, the STFT can be expressed as:

$$\text{STFT}(\tau, f) = \langle x, g_{\tau, f} \rangle = \int x(t) g_{\tau, f}(t) dt = \int x(t) g(t - \tau) e^{-j2\pi f t} dt \quad (7)$$

When we look the Equation 6, we can easily observe that there is a similarity between the frequency modulated of time shifted window function $g(t)$ and the signal $x(t)$. In STFT the time and Frequency resolution can't be assumed arbitrarily and according to the uncertainty principle the product of the time and frequency resolution can be taken as the:

$$\Delta\tau \cdot \Delta f \geq \frac{1}{4\pi} \quad (8)$$

Where $\Delta\tau$ and Δf are time and frequency resolution correspondingly. Analytically the time resolution ($\Delta\tau$) can be defined as:

$$\Delta\tau^2 = \frac{\int \tau^2 |g(\tau)|^2 d\tau}{\int |g(\tau)|^2 d\tau} \quad (9)$$

And, the frequency resolution can be stated as:

$$\Delta\tau^2 = \frac{\int f^2 |G(f)|^2 df}{\int |G(f)|^2 df} \quad (10)$$

Where $G(f)$ is the Fourier transform of $g(t)$

Since there is no guarantee for the selection of a window function for the decomposition of a signal using STFT that's why this inherent drawback motivates the researchers to look for the better solution for the processing of the non-stationary signals.

5.3.3 Wavelet transform: Unlike the STFT technique in which the size of the window is fixed, the wavelet transform performs variable window size.

The wavelet transform of a signal $x(t)$ can be expressed using the notation of the inner product as:

$$wt(s, \tau) = \langle x, \psi_{s,\tau} \rangle = \frac{1}{\sqrt{s}} \int_{-\infty}^{\infty} x(t) \psi^* \left(\frac{t-\tau}{s} \right) dt \quad (11)$$

Where the symbol $s > 0$ represents the scaling parameter and the $\psi^* \left(\frac{t-\tau}{s} \right)$ denotes the scaled Base wavelet. The symbol τ is the shifting parameter. The symbol $\psi^*(t)$ indicates the complex conjugate of the base wavelet $\psi(t)$.

5.4 The wavelet transformation of the signal:

5.4.1 Continuous Wavelet Transform (CWT): In CWT the goal to find the hidden features of a signal the wavelet transform is performed. During this transformation the signal is converted into different forms. The CWT of a signal can be defined as:

$$wt(s, \tau) = \frac{1}{\sqrt{s}} \int_{-\infty}^{\infty} x(t) \psi^* \left(\frac{t-\tau}{s} \right) dt \quad (12)$$

From the definition of CWT it is clear that it is an integral transform.

Properties of Continuous Wavelet Transform:

(a) Superposition property:

If $x(t), y(t) \in L^2(\mathbb{R})$ and c_1 and c_2 are constants. If the CWT of the $x(t)$ is given by $w_{t_x}(s, \tau)$ and that of $y(t)$ is given by $w_{t_y}(s, \tau)$. Then CWT for a given signal $z(t)$ where $z(t) = c_1x(t) + c_2y(t)$ is given by

$$w_{t_z}(s, \tau) = c_1w_{t_x}(s, \tau) + c_2w_{t_y}(s, \tau) \quad (13)$$

Then

$$\begin{aligned} w_{t_z}(s, \tau) &= \frac{1}{\sqrt{s}} \int_{-\infty}^{\infty} z(t) \psi^* \left(\frac{t-\tau}{s} \right) dt \\ &= \frac{1}{\sqrt{s}} \int_{-\infty}^{\infty} [c_1x(t) + c_2y(t)] \psi^* \left(\frac{t-\tau}{s} \right) dt \\ &= \frac{1}{\sqrt{s}} \int_{-\infty}^{\infty} [c_1x(t) + c_2y(t)] \psi^* \left(\frac{t-\tau}{s} \right) dt \end{aligned} \quad (14)$$

(b) Covariant Under translation:

If the CWT of $x(t)$ is $w_{t_x}(s, \tau)$ then the CWT of $x(t - t_0)$ is $w_{t_x}(s, \tau - t_0)$.

(c) Covariant under dilation:

If the CWT of the $x(t)$ is $w_{t_x}(s, \tau)$ then the CWT of $x\left(\frac{t}{a}\right)$ is $\sqrt{a}w_{t_x}\left(\frac{s}{a}, \frac{\tau}{a}\right)$.

(d) Moyal principle:

Let's suppose that if $x(t), y(t) \in L^2(\mathbb{R})$ and the CWT of the $x(t)$ is given by $w_{t_x}(s, \tau)$ and that of $y(t)$ is given by $w_{t_y}(s, \tau)$: that is,

$$w_{t_x}(s, \tau) = \langle x(t), \psi_{s,\tau}(t) \rangle \quad (15)$$

$$wt_y(s, \tau) = \langle y(t), \psi_{s,\tau}(t) \rangle \quad (16)$$

Then,

$$\langle wt_x(s, \tau), wt_y(s, \tau) \rangle = C_\psi \langle x(t), y(t) \rangle \quad (17)$$

Where; $C_\psi = \int_0^\infty \frac{|\Psi(f)|^2}{f} df$, here $\Psi(f)$ indicates the Fourier transform of “ ψ ”.

Some commonly used Wavelets:

(a) Mexican Hat wavelets:

The Mexican Hat Wavelet is defined as that it is a normalized, second derivative of a Gaussian function; which can be mathematically defined as:

$$\psi(t) = \frac{1}{\sqrt{2\pi\sigma^3}} \left(1 - \frac{\sigma^2}{t^2}\right) e^{-\frac{t^2}{2\sigma^2}} \quad (18)$$

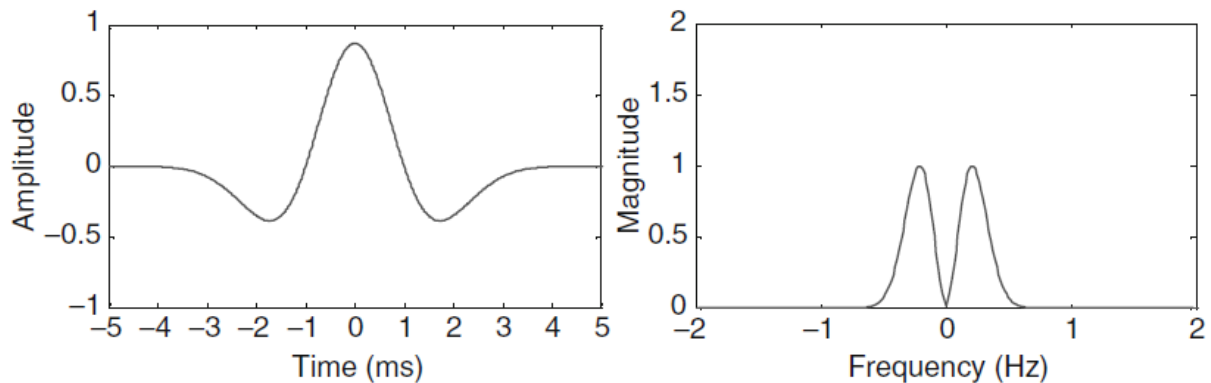


Figure 9-Mexican Hat Wavelet (left) and its magnitude (right)[53].

(b) Morlet wavelet: The Morlet wavelet have been defined as:

$$\psi_M = \frac{1}{\sqrt{\pi f_b}} e^{j2\pi f_c t} e^{-\frac{t^2}{f_b}} \quad (19)$$

Where f_b is the Bandwidth parameter and f_c is the wavelet center frequency.

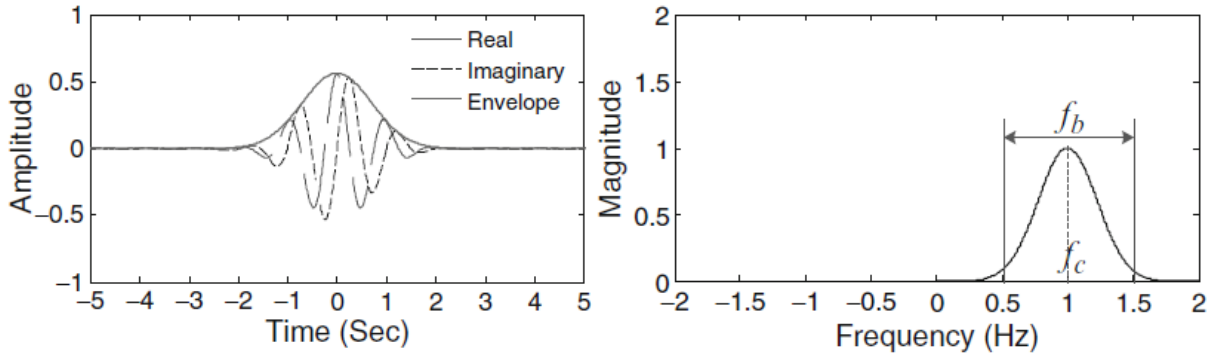


Figure 10-Morlet wavelet (left) and its magnitude spectrum (right); $f_b = 1$ Hz and $f_c = 1$ Hz[53].

(c)Gaussian wavelet:

The Gaussian spectrum can be mathematically expressed as:

$$f(t) = e^{-jt} e^{-t^2} \quad (20)$$

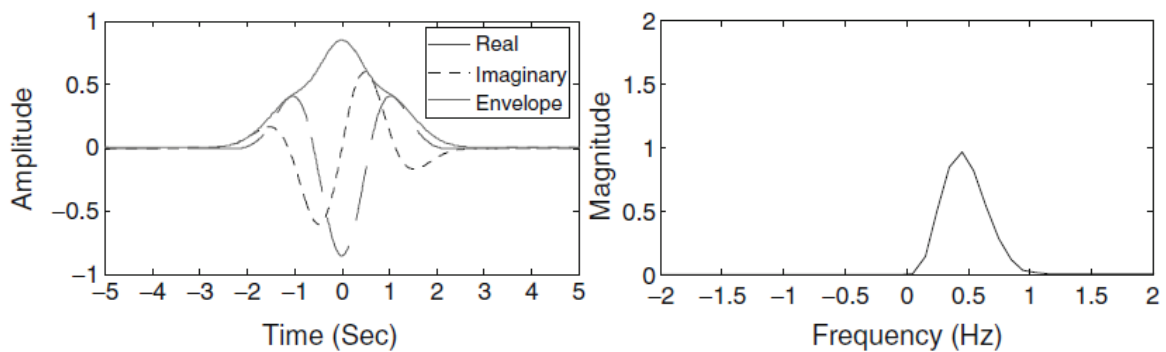


Figure 11-Gaussian wavelet (left) and its magnitude spectrum (right): $N=2$ [53].

(d)Frequency B-spline wavelet:

A frequency B-spline wavelet is defined as:

$$\Psi_b = \sqrt{f_b} \left[\text{sinc} \left(\frac{f_b t}{p} \right) \right]^p e^{j2\pi f_c t} \quad (21)$$

Where f_b is the bandwidth parameter, f_c is bandwidth central frequency and p is integer parameter (≥ 2). Here the function sinc can be defined as:

$$\text{sinc}(x) = \begin{cases} 1 & x = 0 \\ \frac{\sin x}{x} & \text{otherwise} \end{cases} \quad (22)$$

For an example in the case of $f_b = 1\text{ Hz}$ and $f_c = 1\text{ Hz}$ and $p = 2$, the B-spline function is shown in the figure 12.

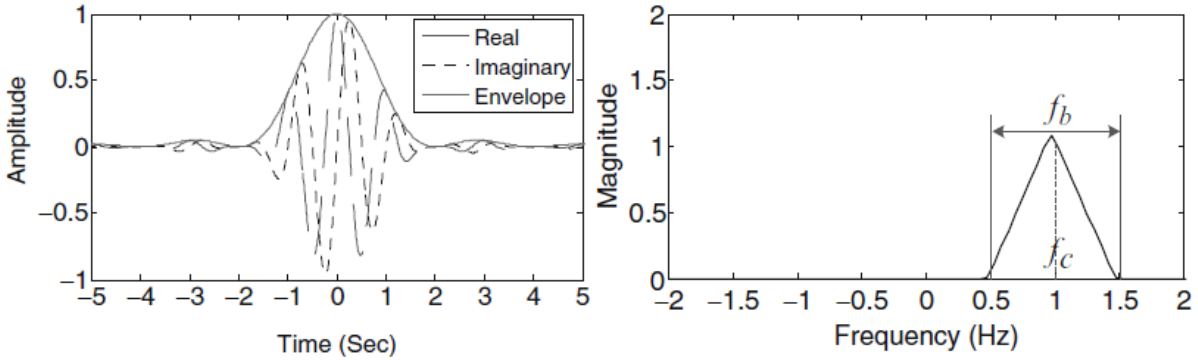


Figure 12-Frequency B-spline wavelet (left) and its corresponding magnitude spectrum (right): $p = 2$, $f_b = 1\text{ Hz}$, and $f_c = 1\text{ Hz}$ [53].

(e) Shannon wavelet: Shannon wavelet is one specific kind of the frequency B-spline wavelet where $p = 1$.

$$\Psi_s(t) = \sqrt{f_b} \text{sinc}(f_b t) e^{j2\pi f_c t} \quad (23)$$

For an example in the case of $f_b = 1\text{ Hz}$ and $f_c = 1\text{ Hz}$ the Shannon wavelet and its corresponding magnitude spectrum has been shown in the Figure 13

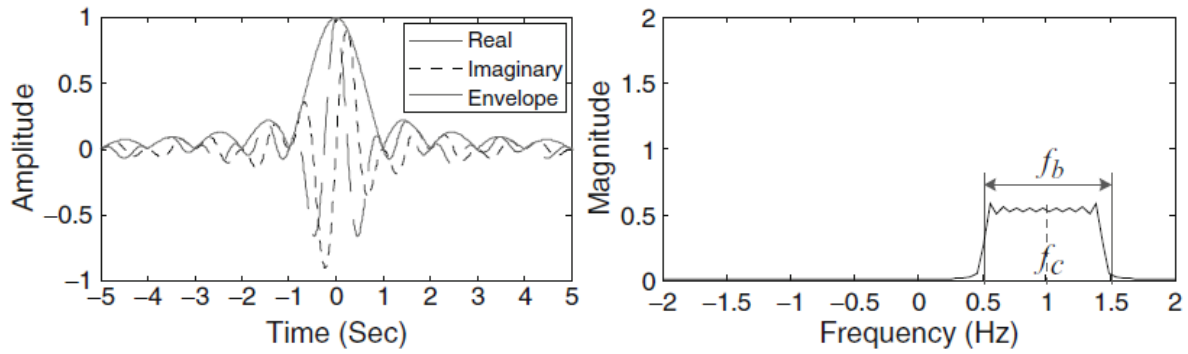


Figure 13-Shannon wavelet (left) and its corresponding magnitude spectrum (right): $f_b = 1$ Hz and $f_c = 1$ Hz [53].

5.4.2 Discrete wavelet transform (DWT): There are two reasons for the adoption of the DWT-(a) To eliminate the redundancy problem which usually happens during CWT. (b) During the experiment the data of a signal are mostly discrete data so the DWT is more preferable for this. The DWT is easier to implement rather than CWT. The main idea of DWT is same as CWT. The DWT provides adequate information for both synthesis of the signal and its analysis as well as it reduces the computation time. Since the computation of the CWT is done by changing the window scale, shifting the window in time along with the multiplication with the signal and integration over the all-time. But in DWT there are cut-off frequencies which are used to analyze the signal on different scales. During this the signal is passed through a high pass filters serially to do the analysis of the high frequencies and it is passed through a series of low pass filters to analyze the low frequencies. The sampling of DWT coefficients is from CWT on a dyadic grid, i.e. $s_0=2$ and $t_0=1$.

The procedure starts when the signal is passed through the half band low pass filter having the impulse response $h[n]$. The filtering operation of a signal corresponds to the mathematical operation of convolution of a signal with the impulse response of a filter. In discrete time the operation of convolution can be defined as:

$$x[n] * h[n] = \sum_{-\infty}^{\infty} x[k]. h[n - k] \quad (24)$$

In a filtering process the low pass filter removes all the frequencies that are above the highest frequency in the signal. The DWT analyzes the signal at different frequency bands by decomposing the signal into a detail information and coarse approximation. In DWT two sets of functions are employed (a) scaling function and (b) wavelet function. The wavelet function corresponds to high pass filter whereas the scaling function corresponds to low pass filter. In DWT the signal is passed through the high pass filter $g[n]$ and a low pass filter $h[n]$. After filtering half the samples can be eliminated by the Nyquist's rule and the highest frequency becomes $p/2$ instead of the p . Thus the subsampling of the signal can be done simply by discarding every other sample.

This can be mathematically expressed as:

$$y[n] = \sum_{k=-\infty}^{\infty} h[k] \cdot x[2n - k] \quad (25)$$

Thus,

$$y_{\text{high}}[k] = \sum_n g[-n + 2k] \cdot x[n] \quad (26)$$

$$y_{\text{low}}[k] = \sum_n h[-n + 2k] \cdot x[n] \quad (27)$$

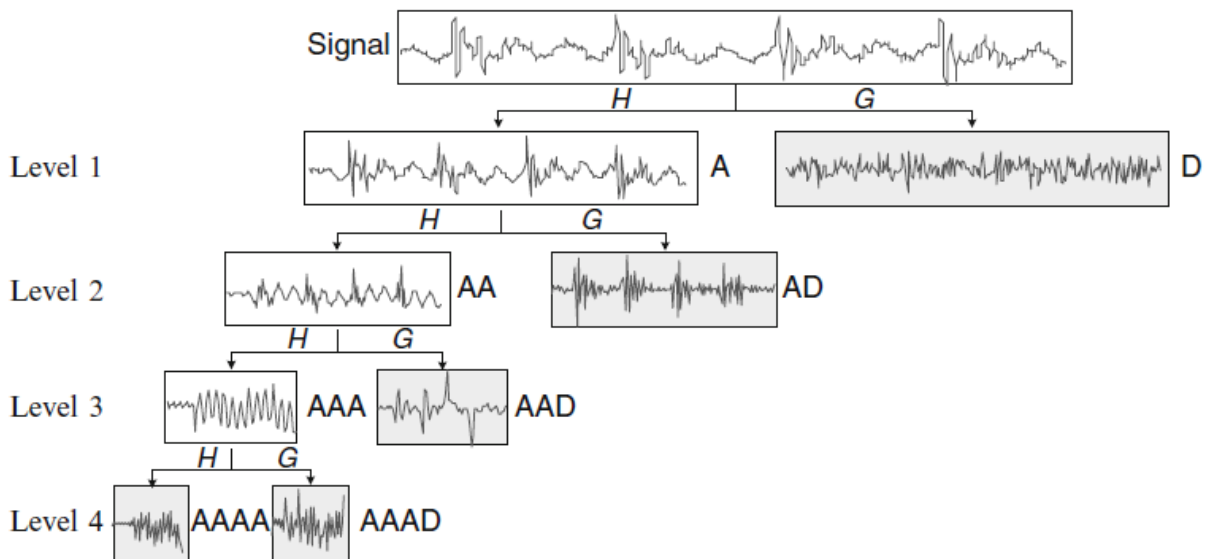


Figure 14-Procedure of a four-level signal decomposition using discrete wavelet transform. Note: H-low-pass filter, G-high-pass filter, A-approximate information, D-detailed information [53].

Therefore the construction formula becomes:

$$x[n] = \sum_{k=-\infty}^{\infty} (y_{\text{high}}[k] \cdot g[-n + 2k]) + (y_{\text{low}}[k] \cdot h[-n + 2k]) \quad (28)$$

5.5 Selection of base wavelet:

There are hundreds of base wavelets in the wavelet analysis. From abundance of base wavelets the selection of appropriate one for a given signal becomes the matter of prime concern. So a different approach has been adopted by different researchers and their approach can be categorized as (a) quantitative and (b) qualitative approach.

5.5.1 Qualitative approach: There are different properties on which the wavelets can be categorized. Some of these properties are symmetry, orthogonality and compact support. If a base wavelet shows the orthogonal property then it means that inner product of the base wavelet with itself will be unity and zero with the other wavelet. Thus the orthogonal wavelet will be quite helpful in the decomposition of the signal into the non-overlapping frequency sub-bands. Another beneficial effect of the orthogonal wavelet is that high computational efficiency can be achieved if the DWT is implemented.

The commonly used base wavelets in DWT are: (a) Haar wavelet (b) Daubechies wavelet (c) Coiflet wavelet (d) Symlet wavelet etc.

(a) Haar wavelet: This is simplest among all the wavelets. It has a linear phase characteristics (i.e. No phase distortion occurs during filtering. It has been used in stamping process monitoring [45] and in the detection of fault in the dry etching process [46].

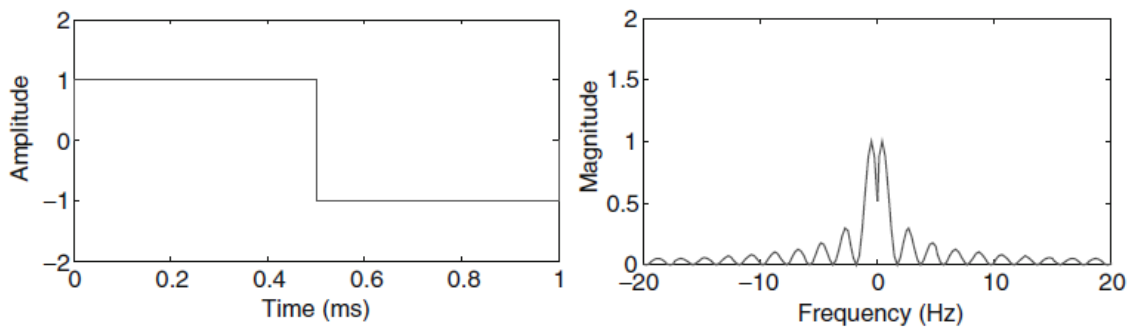


Figure 15-Haar wavelet (left) and its magnitude spectrum (right) [53].

(b) Daubechies wavelet: This wavelet shows the orthogonality but is asymmetric in nature, therefore it can't be used where phase information of the signal needed to be kept.

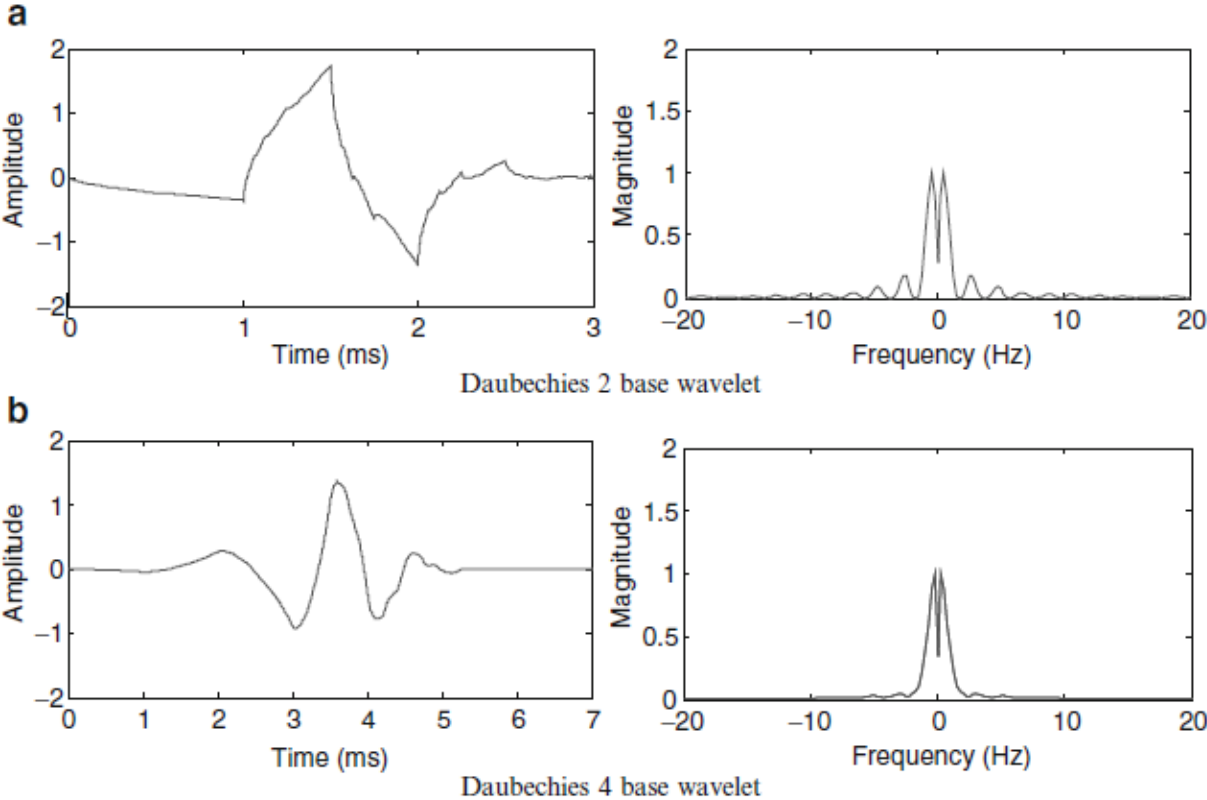


Figure 16-Daubechies wavelet (left) and its magnitude spectrum (right). (a) Daubechies 2 base wavelet and (b) Daubechies 4 base wavelet [53].

It has been up to the order of 20. The Daubechies wavelets have been widely investigated for fault diagnosis of bearings and automatic gears [47].

(c) Couplet wavelet: This wavelet is orthogonal and near symmetric in nature.

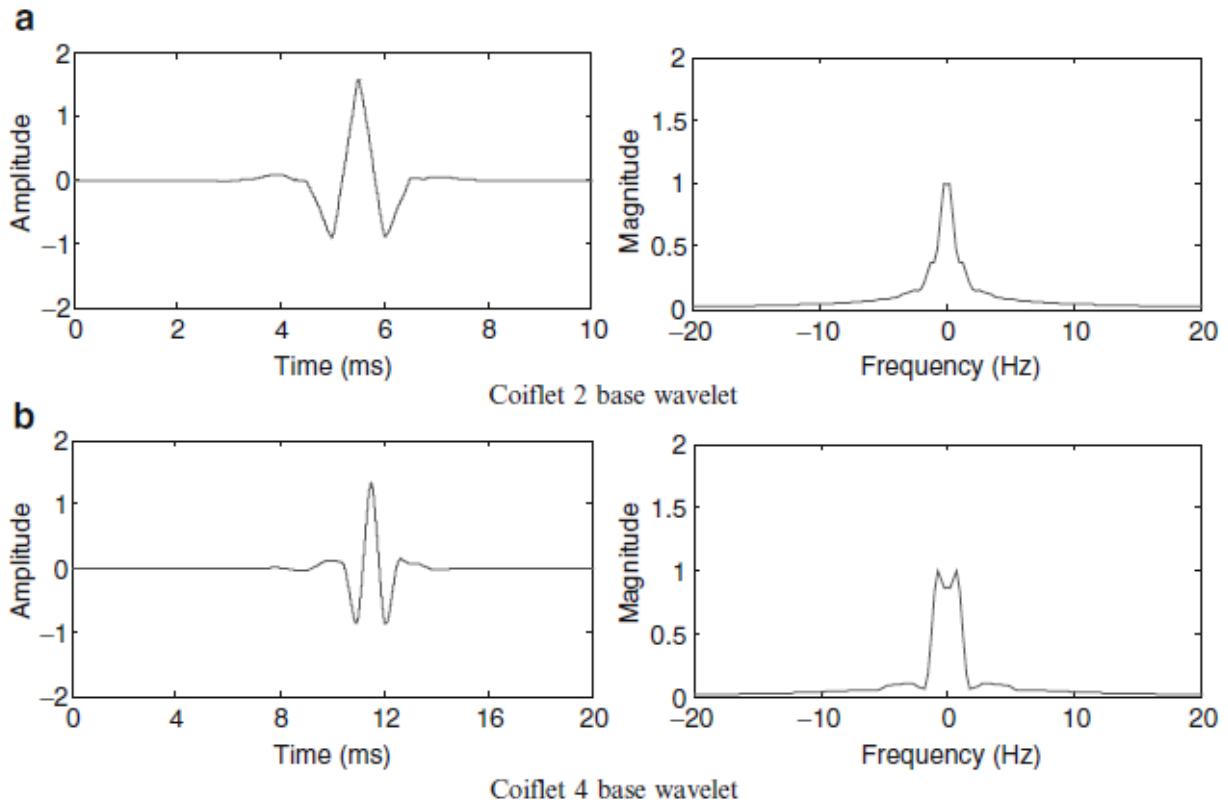


Figure 17-Coiflet wavelet (left) and its magnitude spectrum (right). (a) Coiflet 2 base wavelet and (b) Coiflet 4 base wavelet [53].

(d) Symlet wavelet: Symlet wavelets are orthogonal and near symmetric these properties ensure minimal phase distortion. An example of the application of this wavelet can be seen in health monitoring of the roller bearing.

To act as a linear phase filter the base wavelet should have the symmetry property such that during filtering it couldn't lead to the phase distortion. The compact support is the property of base wavelet which shows that the basis function is zero outside the finite interval and nonzero inside the finite interval. This kind of wavelet allows the efficient representation of the localized features.

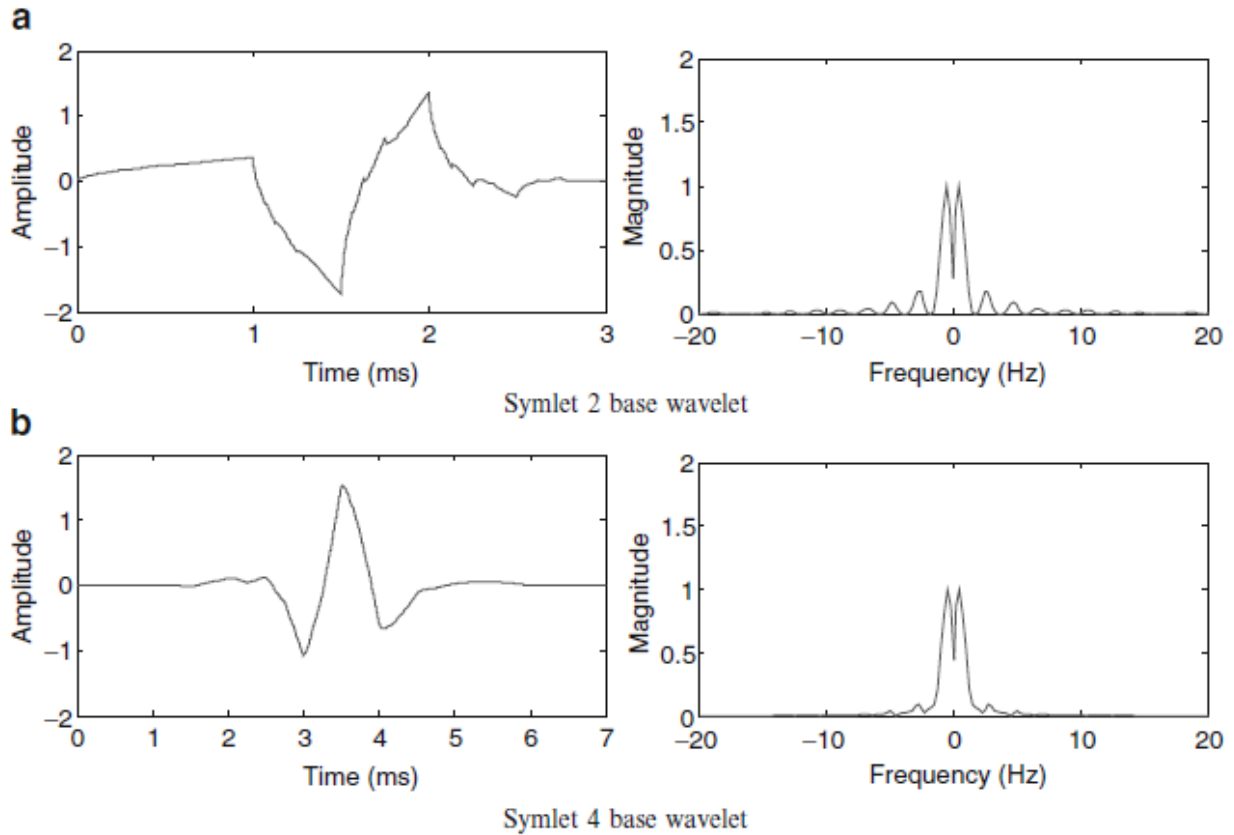


Figure 18-Symlet wavelet (left) and its magnitude spectrum (right). (a) Symlet 2 base wavelet and (b) Symlet 4 base wavelet [53].

During the qualitative analysis for the selection of the base wavelet in the signal it is very difficult to do the visual comparison between the base wavelet and the shape of the signal, that's why the quantitative measures become necessary for the selection of base wavelet to eliminate these deficiencies.

5.5.2 Quantitative approach: The measured quantities of the signal like Shannon entropy, Fishlow's measure, Emelen's modified entropy measure, Schur convex functions etc. were used in the selection of the base wavelet. For e.g. the base wavelet selection had been made using Shannon entropy for the velocity and temperature time series analysis in base wavelet.

5.6 Entropy of a signal:

Entropy gives the measure that how much system is close to equilibrium and the disorder in the system. In the signal analysis Transient feature extraction is an important part which we can obtain using the entropy of the signal. Wavelet entropy is a combination of wavelet decomposition and entropy statistics theories. It allows not only segmentation but clustering also. It defines the number of different Combinations possible that can be obtained in a signal i.e. more random and unpredictable a signal is , the Greater its entropy. In a generalized manner we can say that the entropy measures the disorder of the energy. It gives the measure that in how many ways we can reorganize the system.

The entropy of the signal can be defined using the information theory. To determine the entropy we should first define the Information function (I) in terms of the event I and with probability p_i . Therefore, to get the idea about the information acquired due to the event, i, the following information property is followed by Shannon' solution.

1. If $I(p) \geq 0$ -Information is either zero or positive.
2. $I(1) = 0$ -Event 1 has no information.
3. $I(p_1 p_2) = I(p_1) + I(p_2)$ -Information due to independent event should be additive.

The last property gives the idea that joint probability gives the same amount of information as given by the two separate events. If the first event produces one of the n equiprobable items and second event produces one of the m equiprobable items then here are mn possible outcomes of the joint events. This indicates that $\log_2 n$ bits are required for encoding the first value, $\log_2 m$ bits are required for the second value and $\log_2 mn$ for both values. Where:

$$\log_2 mn = \log_2 n + \log_2 m \tag{29}$$

Shannon discovered that the proper choice of function to quantify information, preserving this additivity, is logarithmic.

According to the definition of the entropy H (Named after Boltzmann's H-theorem) given by the Shannon is that for a discrete random variable X is having possible values (x_1, \dots, x_n) and probability mass function $P(X)$.

$$H(X) = E [I(X)] \tag{30}$$

Where E is the expected value operator and I is the information content of X.

[Note: $E(X) = X_1P_1 + \dots + X_nP_n$]

Since the self-information content of associated with the random variable is synonymous to its entropy.

i.e.

$$I(X; X) = H(X) \tag{31}$$

Where $I(X; X)$ is the mutual information of X with respect to itself.

By definition the amount of self-information is dependent on the probability i.e. smaller the probability of any random variable, larger will be the self-information associated with it and vice versa.

Thus we can write information of X as:

$$I(X) = \log\left(\frac{1}{p(x_i)}\right) \tag{32}$$

Thus

$$\begin{aligned} H(X) &= E\left[\log\left(\frac{1}{p(x_i)}\right)\right] \\ &= E[-\log(p(x_i))] \end{aligned} \tag{33}$$

For finite number of values in the given sample of random variables the entropy can be written as:

$$H(X) = -\sum_i p(x_i)\log_b(p(x_i)) \tag{34}$$

Where b is the base of the logarithm used. Common values of b are 2, Euler's number e, and 10, and the unit of entropy is shannon for $b = 2$, nat for $b = e$, and hartley for $b = 10$.

5.7 Energy of a signal:

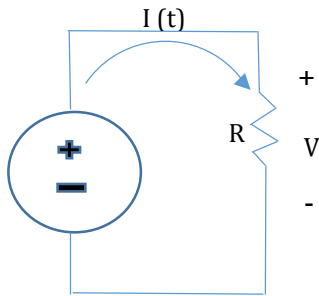


Figure 19-Electric circuit

The Figure 19 is a simple electrical circuit where there is a resistor of resistance (R), the voltage across the resistor (V) and the current going through the resistor (I). In this case the voltage and the current are the functions of time. In this case the power generation in the circuit is P .

From the circuit analysis the power generation can be written as:

$$P = \frac{V^2(t)}{R} = I^2(t) \cdot R \quad (35)$$

As for the above case we can conclude that

$$P \propto V^2(t) \quad (36)$$

And

$$P \propto I^2(t) \quad (37)$$

From the signal processing or the signals in the system it is observed that for any arbitrary signal $X(t)$ the power is equal to $|X(t)|^2$. In system we typically talk about the magnitude of the signal and the power of the signal but in reality there is no power dissipated by the signal themselves like the mechanical or electrical. But this can be used symbolically for the analysis of the processes using different kind of signal like voltage current etc.

Since the power is Energy per unit time, therefore Energy (E) of a signal of infinite period can be represented as:

$$E = \int_{-\infty}^{\infty} |X(t)|^2 dt \quad (38)$$

In some cases the system shows the finite energy and in some cases there are infinite energy in a given signal of infinite period. Therefore the Average power (P_{avg}) of the signal is calculated which can be written as:

$$P_{avg} = \lim_{T \rightarrow \infty} \frac{1}{T} \int |X(t)|^2 dt \quad (39)$$

During the analysis of the Discrete random variable values of a signal $X(x_1, \dots, x_n)$ the Energy of the signal can be written as:

$$E = \sum_{i=1}^n |x_i|^2 \quad (40)$$

5.8 Wavelet energy entropy (WEE):

The Wavelet energy entropy is a combination of information entropy and wavelet energy spectral analysis. In this the probability distribution sequence is the sequence of wavelet coefficient matrix. This is based on the multi scales and it can be calculated according to the reconstructing of wavelet coefficients. The harmonics in the power system has a characteristics that less than 17 times the harmonics is considered as steady state harmonics and more than 17 times is considered as transient harmonics. We can analyze the signal using the wavelet energy entropy in a fixed time window. Let E_1, E_2, \dots, E_n be the wavelet energy spectrum of n decompositions. Thus from the properties of orthogonal wavelet total power E will be equal to the sum of energy at all decomposition level i.e. ($E = E_1 + E_2 + \dots + E_n$) Let Energy probability density distribution $p_j = E_j/E$ then $\sum_j P_j = 1$. therefore the wavelet energy entropy (WEE) can be correspondingly defined as follows.

$$W_{EE} = - \sum_j p_j \log p_j \quad (41)$$

In the formulae given above, $E_j = - \sum_k |D_j(k)|^2$

5.9 Criteria for the wavelet selection: The wavelet selection is based upon the qualitative analysis and quantitative analysis. The criteria for wavelet selection have been discussed in detail in chapter 6.

Chapter 6

Results and discussion

6.0 Overview:

This chapter contains two parts. The first part deals with the Wavelet analysis of the current signals. The last part deals with the HAZ Hardness analysis.

6.1 Wavelet analysis:

Wavelet analysis gives the time-frequency representation and de-noising of the signal [53]. This analysis has wide application like Signal processing, Data compression, Smoothing and image de-noising, Fingerprint verification, DNA analysis, protein analysis, Biology for cell membrane recognition, to distinguish the normal from the pathological membranes, Blood-pressure, heart-rate and ECG analyses, Finance (which is more surprising) for detecting the properties of quick variation of values, in Internet traffic description, for designing the services size, Industrial supervision of gear-wheel, Speech recognition, Computer graphics and multi-fractal analysis, etc. It is quite useful for application because it De-noises and compresses the signal without any appreciable degradation. Analysis of non-stationary signals can be done and Simultaneous localization in time and frequency domain is possible. It is computationally very fast and it does the good approximation of the any given function f . Wavelet theory is capable of revealing aspects of data that other signal analysis techniques miss the aspects like trends, breakdown points, and discontinuities in higher derivatives and self-similarity.

6.1.1 Criteria for the Wavelet selection:

The selection of Base wavelet which is best suited for analysis is very much important and it can be done in two ways (a) by Qualitative measure and (b) by Quantitative measure. During Qualitative measure Base wavelets are characterized by different properties like Orthogonality, Symmetry and Compact support. By using Orthogonality we can find better decomposition of signal which don't overlap and for filtration in linear phase Symmetry property is useful. To efficiently represent the localized feature of the signal the compact support wavelet is used. The investigation of these properties can give the idea of selection of Base Wavelet but literature suggests to do the Quantitative analysis for the selection of best Base Wavelet because accurate match of the shape of signal and base wavelet is difficult. There are different criteria suggested like Maximum Energy criteria, Minimum Shannon-Entropy criteria etc. But the Energy-to-Shannon Entropy ratio measure has been considered

the most suitable criteria to select the appropriate wavelet for the transient Signal analysis [53].

The Energy content of the signal is the measure which uniquely characterizes it. The Energy content of a signal $\chi(t)$ can be expressed as:

$$E_{\chi(t)} = \int |\chi(t)|^2 dt \quad (42)$$

Similarly, if signal has discrete sample values $\chi(i)$ ($i=1,2,\dots,N$), then Energy ($E_{\chi(i)}$) can be written as:

$$E_{\chi(i)} = \sum_{i=1}^N |\chi(i)|^2 \quad (43)$$

The Energy distribution is quantitatively described by the Shannon Entropy (H_{Shannon}) and this can be Expressed as:

$$H_{\text{Shannon}} = - \sum_{i=1}^N P_i \log_2 P_i \quad (44)$$

Where P_i is the energy probability distribution of the wavelet coefficients, defined as :

$$P_i = \frac{|\text{wt}(s,i)|^2}{E_{\chi(i)}} \quad (45)$$

Where $\text{wt}(s, i)$ denotes the wavelet coefficient and N is the number of Wavelet coefficients.

Since the selection of Base wavelet can be done by Maximum Energy criteria or by the Minimum Shannon Entropy criteria but if the ratio of Maximum Energy to Minimum Shannon entropy is found out then it can give better outcome than the above both criteria. The Energy to Shannon Entropy ratio $R(s)$ of the signal can be defined as:

$$R(s) = \frac{E_{\chi(i)}}{H_{\text{Shannon}}} \quad (46)$$

The wavelet giving the maximum $R(s)$ value is selected for the transformation of the signal. In our analysis we have taken discrete samples of the signal and it has been tried to find the energy-entropy ratio first.

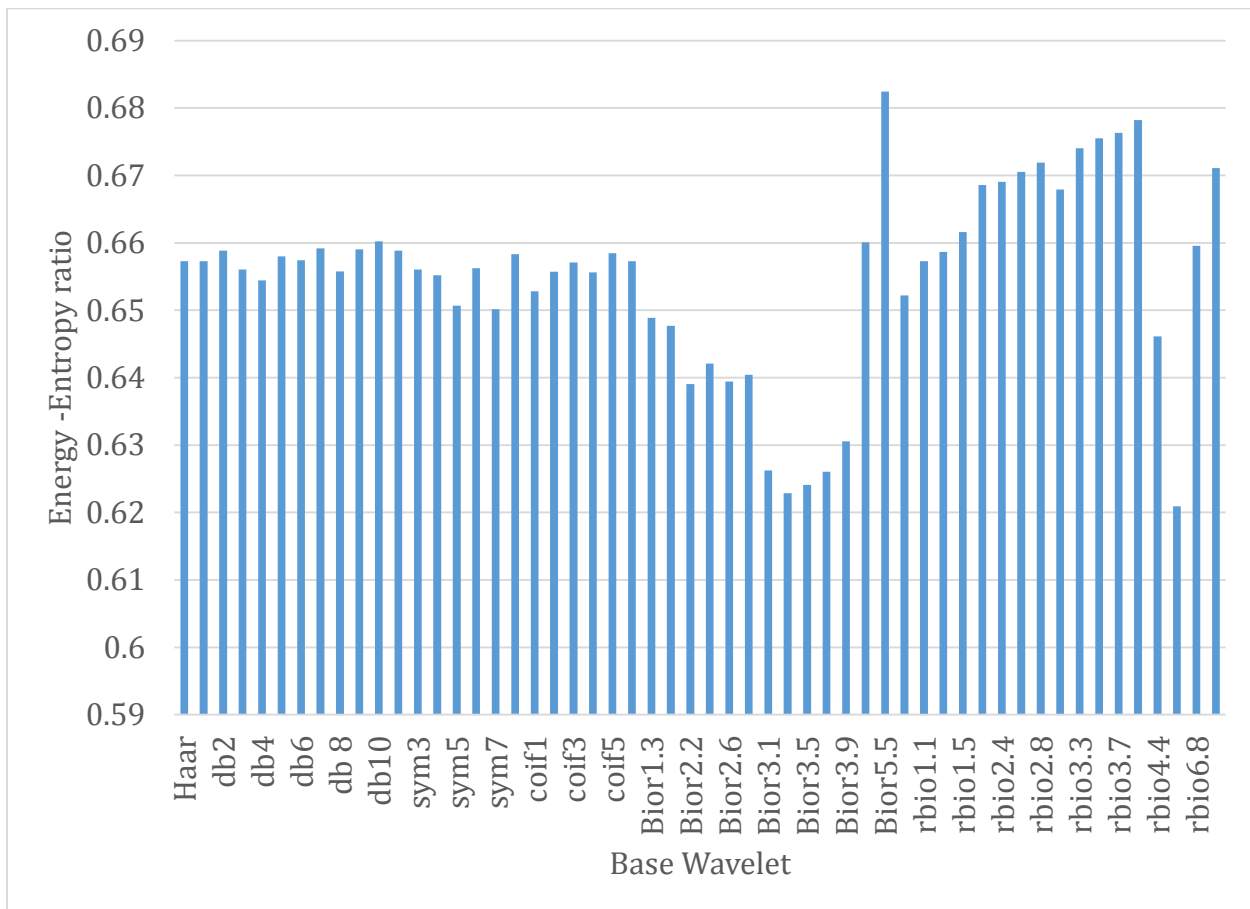


Figure 20-Energy-entropy ratio for different Basewavelet.

After finding the $R(s)$ using different base wavelets it is observed that Bior5.5 gives the maximum value as shown in the Figure 20 for a given signal. Therefore base wavelet Bior5.5 has been used for the Entropy analysis of all the signals.

6.1.2 Signal Entropy analysis

The Entropy of a signal gives the information about the randomness in it. Lesser the value of Entropy indicates the more stability of a signal in comparison with the signal having a higher entropy value. Li et al. [54] have shown that the wavelet energy entropy can be used as an arc stability evaluation criteria in arc welding. They have shown that the higher value of wavelet energy entropy, lesser the stability of arc is and vice-versa.

This subsection has been further divided into two parts. The first part deals with the wavelet energy entropy analysis of the lead and trail current signals for the set of experiments having different current combinations with different types of electrode diameter combinations. The last section deals with the wavelet energy entropy analysis of a set of experiments having Equal current with different types of electrode diameter combinations.

6.1.2.1 Comparative study of arc stability for equal and unequal currents in the lead and trail using wavelet energy entropy.

This section deals with the wavelet energy entropy analysis of the set of experiments given in the Table 6.

The Figure 21 depicts the bar chart of the wavelet energy entropy of different combinations of lead and trail current.

This graph has been plotted for the 0.8-0.8mm diameter of the lead-trail in which the data have been collected as per the rate of thousand data per second. From the graph it can be observed that when lead current and trail current are equal in magnitude then the trail achieves the maximum entropy level and Lead also attains a large entropy value. This signifies that the equatorial current in Lead and trail causes the maximum instability in an arc. Further, we can observe that when we increase the trail current by keeping lead current constant, then the entropy of the trail varies, but there is almost very minimal effect on the lead entropy level. But when the lead current is increased then the entropy of lead as well as trail both decreases. This shows that the stability of the arc increases when we increase the difference between lead and trail. When the lead current is more than the trail current and the difference between the lead and trail is maximum than the stability will be maximized. This result matches nicely with the results of Moinnuddin and Sharma [25].

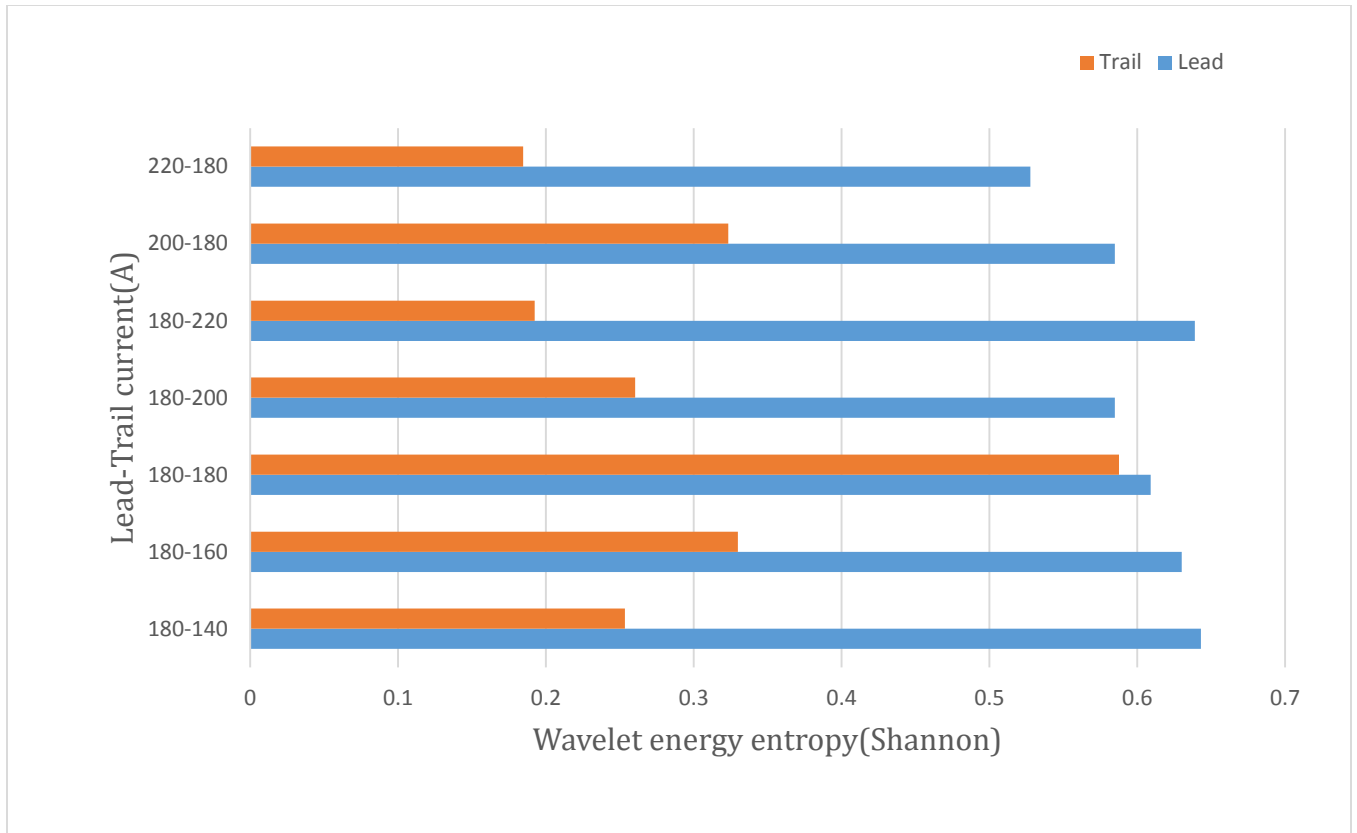


Figure 21 -WEE of lead and trail current for 0.8-0.8mm wire diameter combination.

The Figure 22 shows the bar chart of the wavelet energy entropy of a set of experiments in which the lead-trail wire diameter is 0.8-1.2mm. From the Figure 22 it can be observed that when we increase the trail current by keeping the lead current constant then there is very little variation in the entropy of the lead as well as trail but when trail current becomes very-very large then the trail achieves comparatively most stable state. But there is not a significant change in the wavelet energy entropy of lead has been achieved.

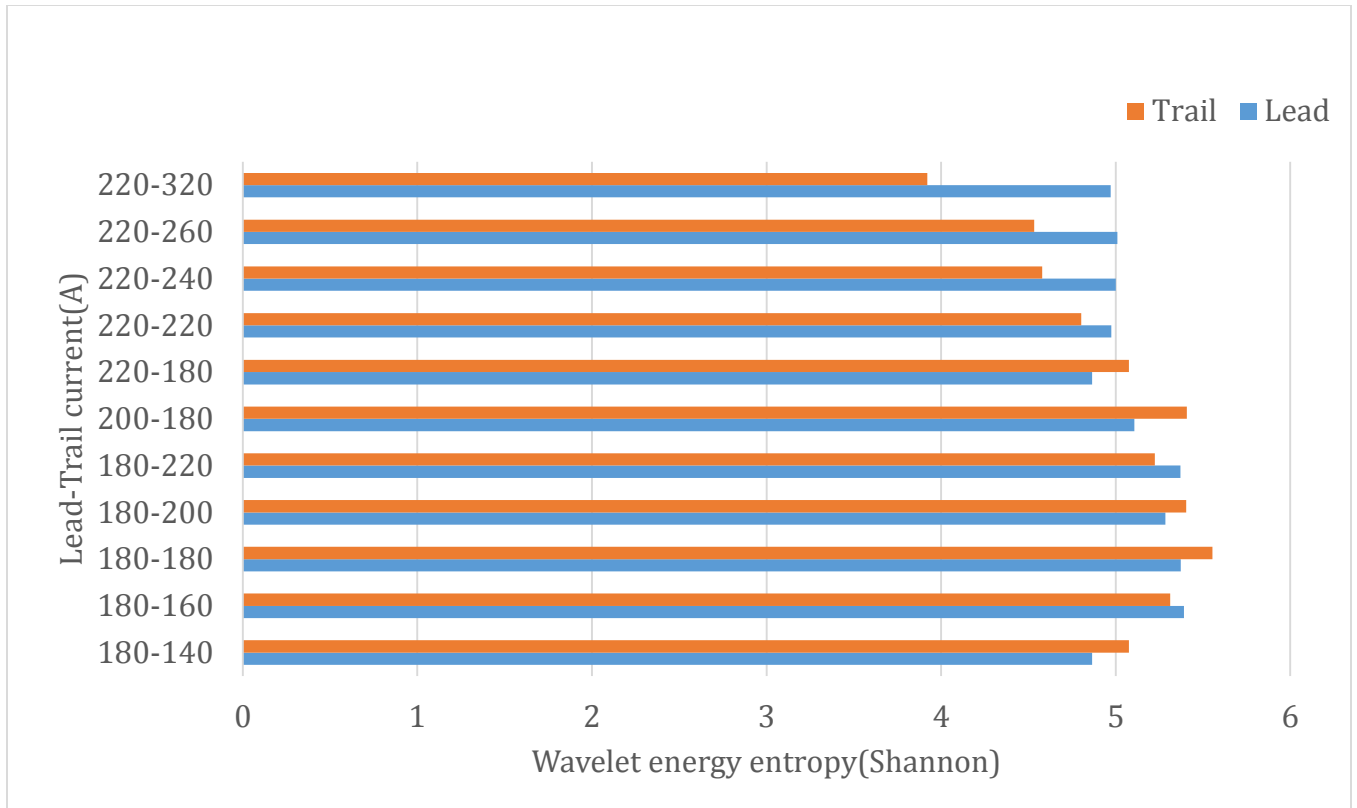


Figure 22 -WEE of lead and trail current for 0.8-1.2mm wire diameter combination.

The Figure 23 shows the bar chart of the set of experiments given in the Table 6. In which the lead-trail wire diameter has been taken as 1.2-0.8mm. From the graph it can be observed that when we increase the trail current by keeping lead current constant, then the stability of trail increases, but there is very small change in the stability of the lead. But when we increase the lead current by keeping trail current constant, then with the increase in the difference between lead and trail the stability of the arc increases significantly.

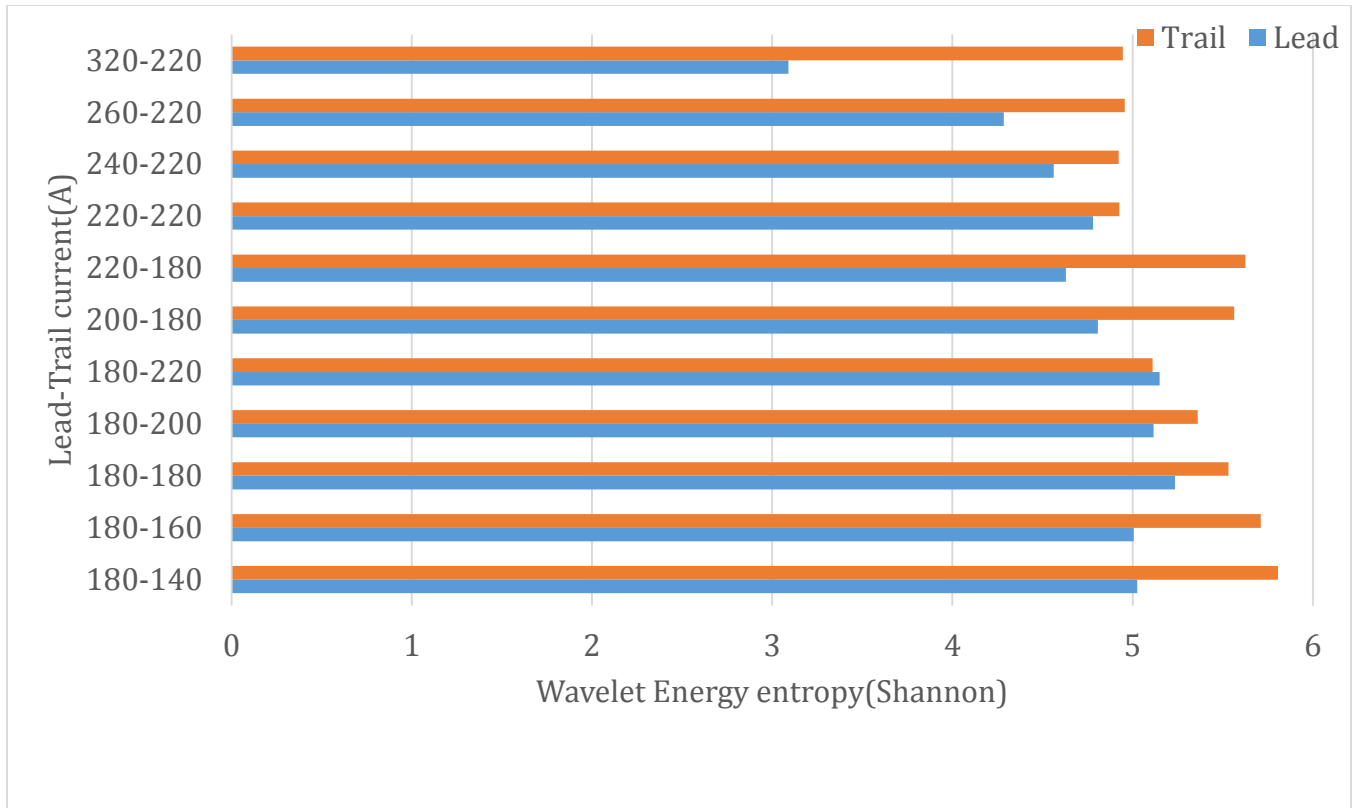


Figure 23 -WEE of lead and trail current for 1.2-0.8mm wire diameter combination.

6.1.2.2 Wavelet energy entropy analysis for Equal current with different types of electrode diameter combinations.

This section deals with the wavelet energy entropy analysis of the set of experiments given in the Table 6. In this the lead and trail currents are equal for all the cases.

The Figure 24 depicts the bar chart of the wavelet energy entropy for the 0.8-0.8mm lead-trail diameter condition. From the Figure it can be observed that when we increase the current in the lead and trail by keeping them equal, then the wavelet energy entropy of the arc decreases. But the decrement is very small when compared with the dissimilar current cases. This indicates that the stability of the arc increases with increases in current but it has not a much significant effect.

The Figures (25, 26, and 27) show the bar chart of the set of experiments of equal current condition in which corresponding diameter combinations are 1.2-0.8mm, 1.2-1.2mm and 0.8-1.2mm. From these figures we can observe that for higher current values the wavelet

energy entropy of the current signals is comparatively smaller. Which signifies the increase in the stability of arc in higher current value condition.

From the Figures (25 and 27) it can be observed that the WEE of lead and trail decreases more significantly when compared to the similar diameter condition. This shows that in the case of equal current and different wire diameter combinations the arc stability will increase more significantly with an increase in current when compared to the similar diameter case.

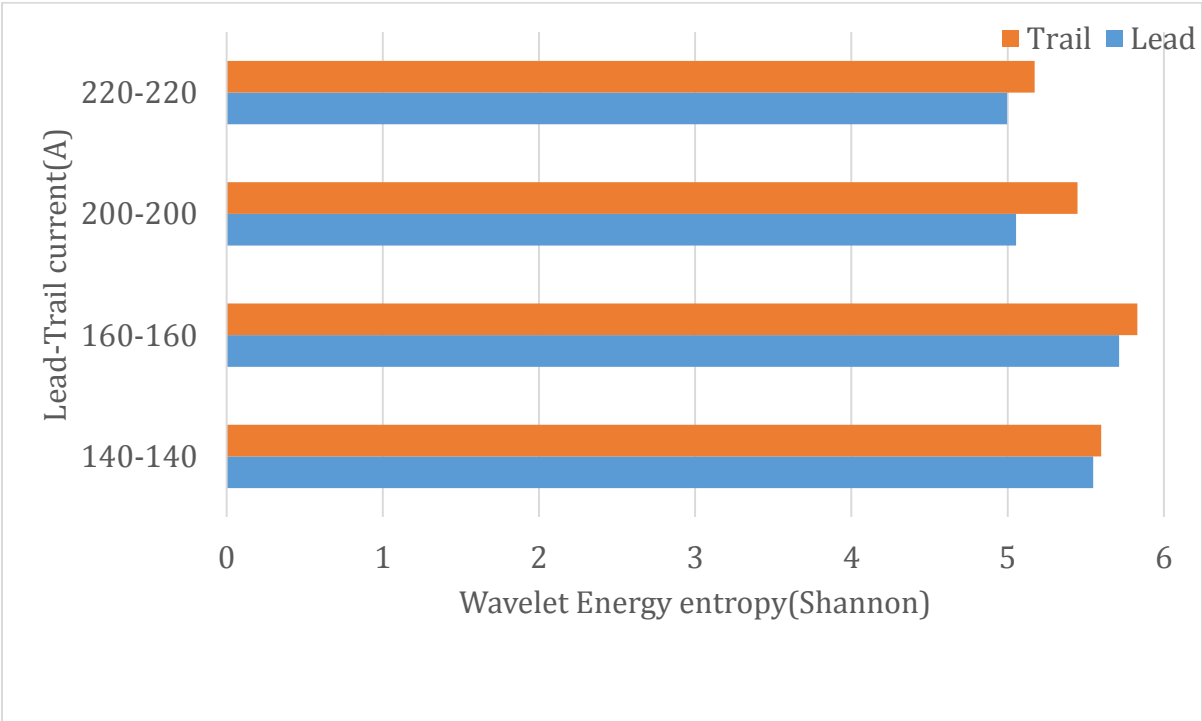


Figure 24-WEE for equal current and 0.8-0.8mm wire diameter combination.

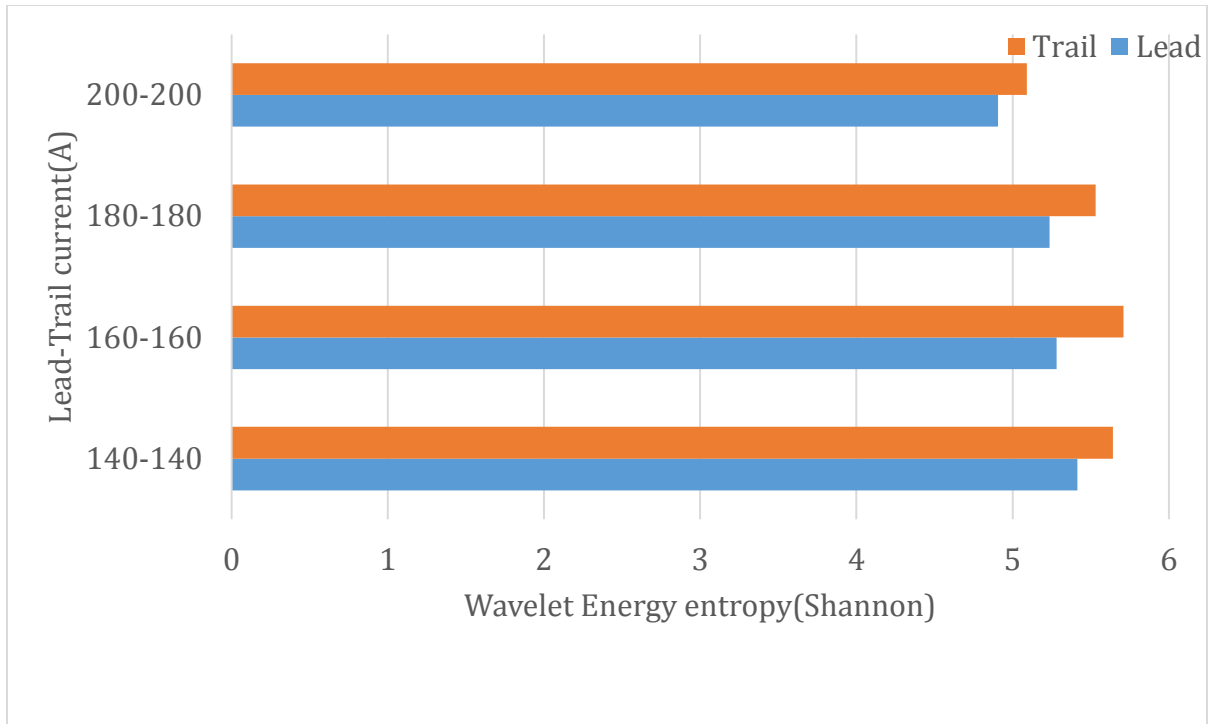


Figure 25-WEE for equal current and 1.2-0.8mm wire diameter combination.

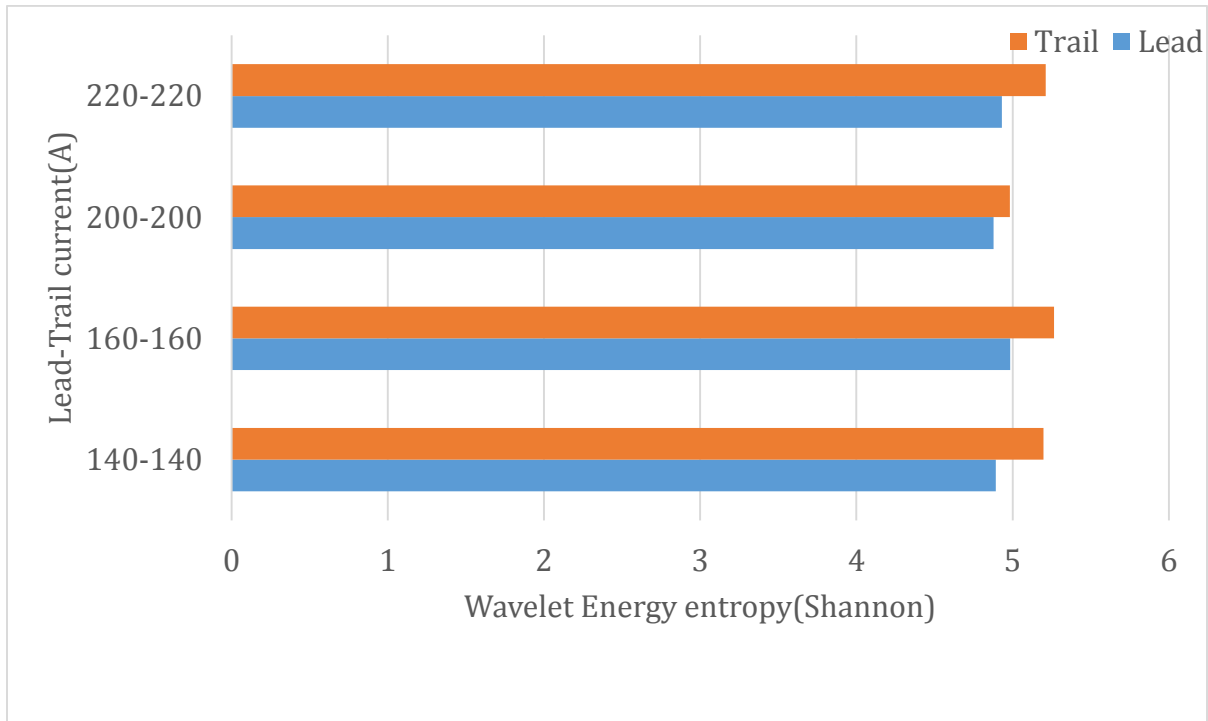


Figure 26-WEE for equal current and 1.2-1.2mm wire diameter combination.

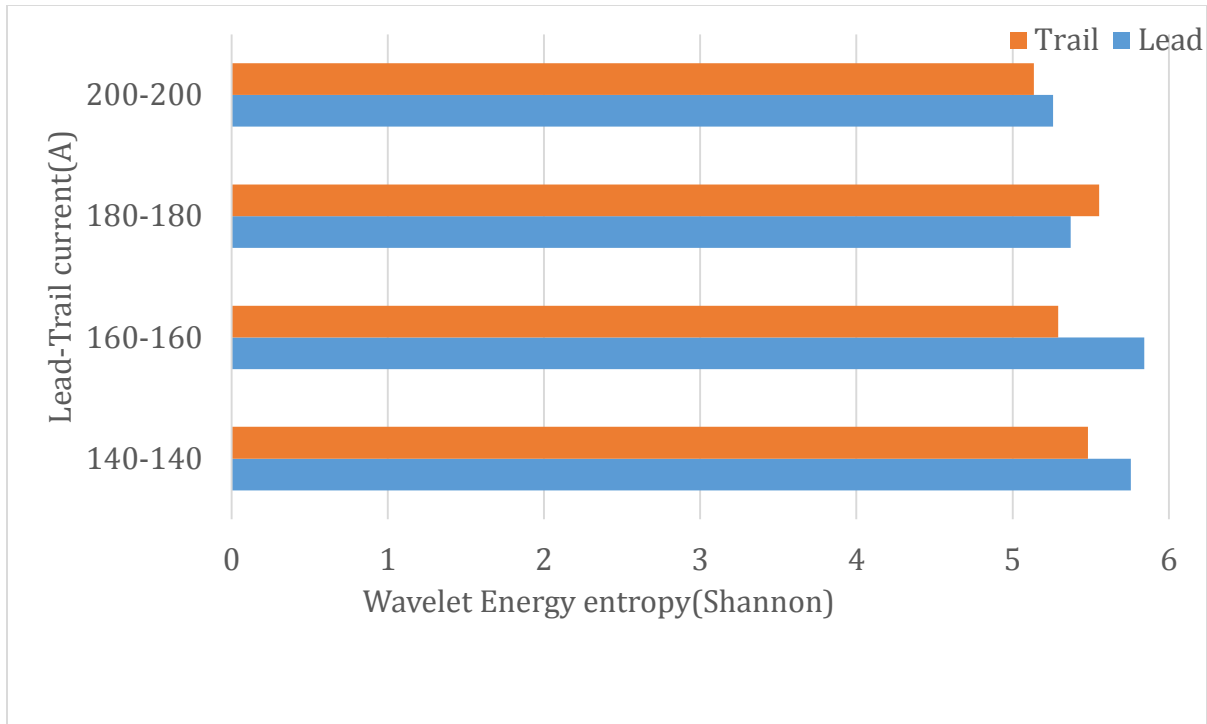


Figure 27-WEE for equal current and 0.8-1.2mm wire diameter combination.

According to Sharma et al. [9] the current density of lead and trail current plays a major role in the stability of arc. According to them if the lead current density is more than the trail current density, then the arc will be more stable. The Figure 28 shows the WEE of the lead and trail with respect to the difference of lead and current density for the set of experiments given in the Table 6. In the Figure 28 a second degree polynomial curve has been fitted. From the figure it is quite clear that when the difference of lead and current density is zero, then it attains the maximum WEE value in lead and trail. But when this difference attains a negative or positive value, then the stability increases. But if the difference of current intensity is positive, then the stability will be maximized when compared to the negative value.

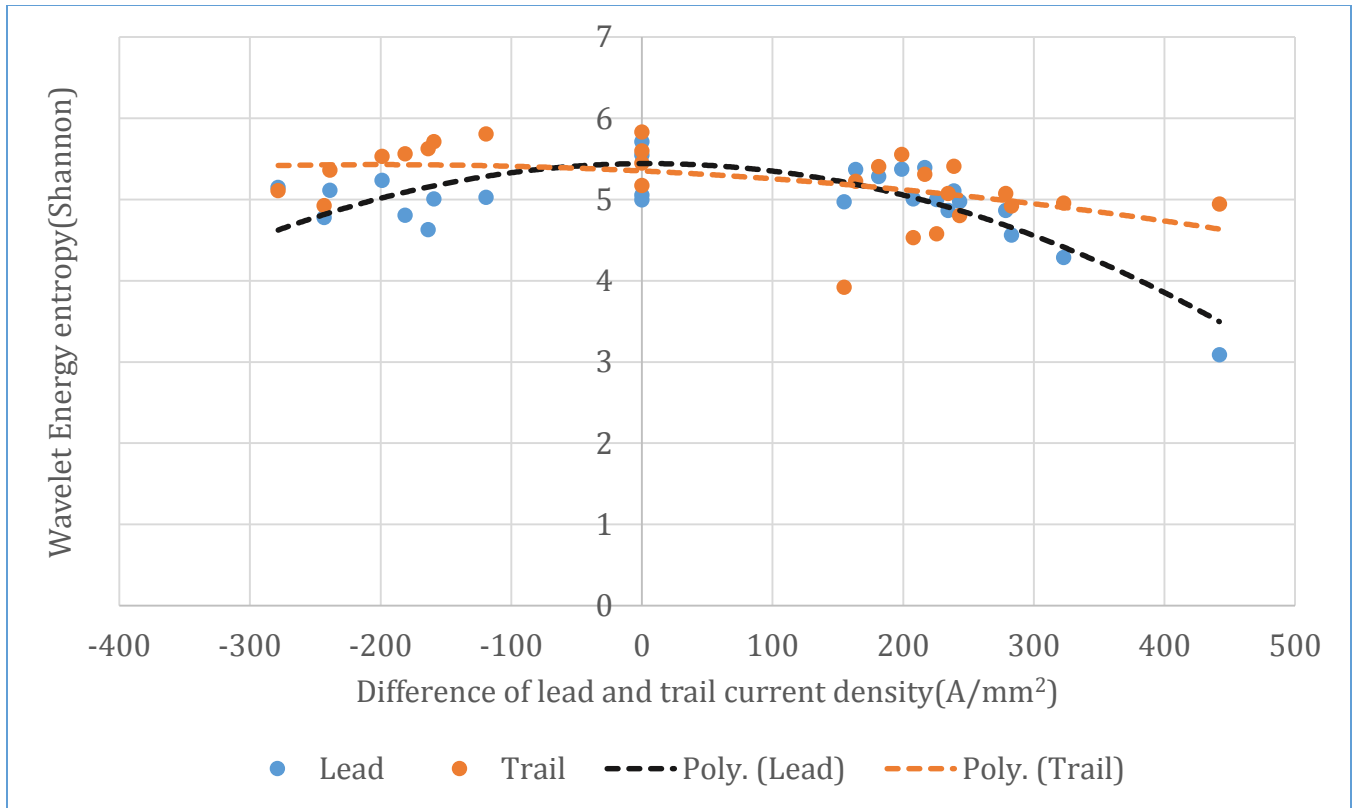


Figure 28-WEE v/s current density difference graph.

6.2 HAZ (Heat affected zone) Hardness analysis:

Hardness is the resistance to indentation. It is the property which gives resistance to permanent deformation. Higher the hardness value indicates the high resistance for indentation. Hardness of a material depends on its toughness, elastic and plastic properties. Mainly there are three types of hardness measurement. They are as follows:

- **Scratching:**

Scratch hardness is how much material is resistant to fracture from the sharp object. A harder material is used to scratch. Based on the force required to scratch gives the hardness of the object. The most common scale used to test are Mohs scale and pocket hardness tester.

- **Indentation:**

In indentation process continuously compressive load is applied with the help of a sharp object. The tests work on the basic premise of measuring the critical dimensions of an indentation left by a specifically dimensioned and loaded indenter.

- **Rebound:**

It is also known as dynamic hardness. In this a diamond tipped hammer is made to fall down. Based on the range it bounces back decides the hardness. This test is depends on the elastic property of material.

Hardness is the property of a material that enables it to resist plastic deformation, usually by penetration. However, the term hardness may also refer to resistance to bending, scratching, abrasion or cutting. As each metal is made up of number of molecules, the bond between these molecules decides the hardness of the metal. As it is possible to mix the materials the interstitial atoms occupies vacant space between the atoms. It results into increase in the hardness of material. By varying the density of dislocation and presence of interstitial atoms, hardness of a material can be varied.

In this section the HAZ hardness for the set of experiments have discussed which are given below:

6.2.1 HAZ Hardness analysis of equal and unequal current condition with different wire diameter combination:

Hardness is the material property which depends on the microstructures of the material. The hardness of a welded material depends on the welding conditions like amount of Heat input and its concentration, cooling method etc. When we check the hardness of the welded material then it is found that there is a sudden change in the hardness in the HAZ zone [53]. Moinnuddin and Sharma [25] have shown that when the difference between the lead and trail current ($I_L - I_T$) is zero then the HAZ Hardness is maximum with respect to other cases. The hardness decreases with the increase in the difference of lead current and trail current and when the lead current is more than the trail current then the least HAZ Hardness is found. This shows that the HAZ Hardness is dependent on the stability of the arc. Since in the

stable arc condition there is a proper input of heat and this effect the microstructure of the weldment. If the arc is not stable then it will spread and the surface hating will occur and it will be helpful in increasing the surface hardness rather than changing the microstructure.

The Figure 29 shows the bar chart of HAZ Hardness of the specimen of the set of experiments given in the Table 6. This experiment has been done with similar and dissimilar currents in lead and trail and the lead-trail wire diameter has been taken as 0.8-0.8mm. From the figure it can be observed that the maximum HAZ Hardness has been achieved when the lead and trail currents are equal. The least HAZ Hardness has been achieved when the difference between the lead and trail current is maximum and lead current is more than the

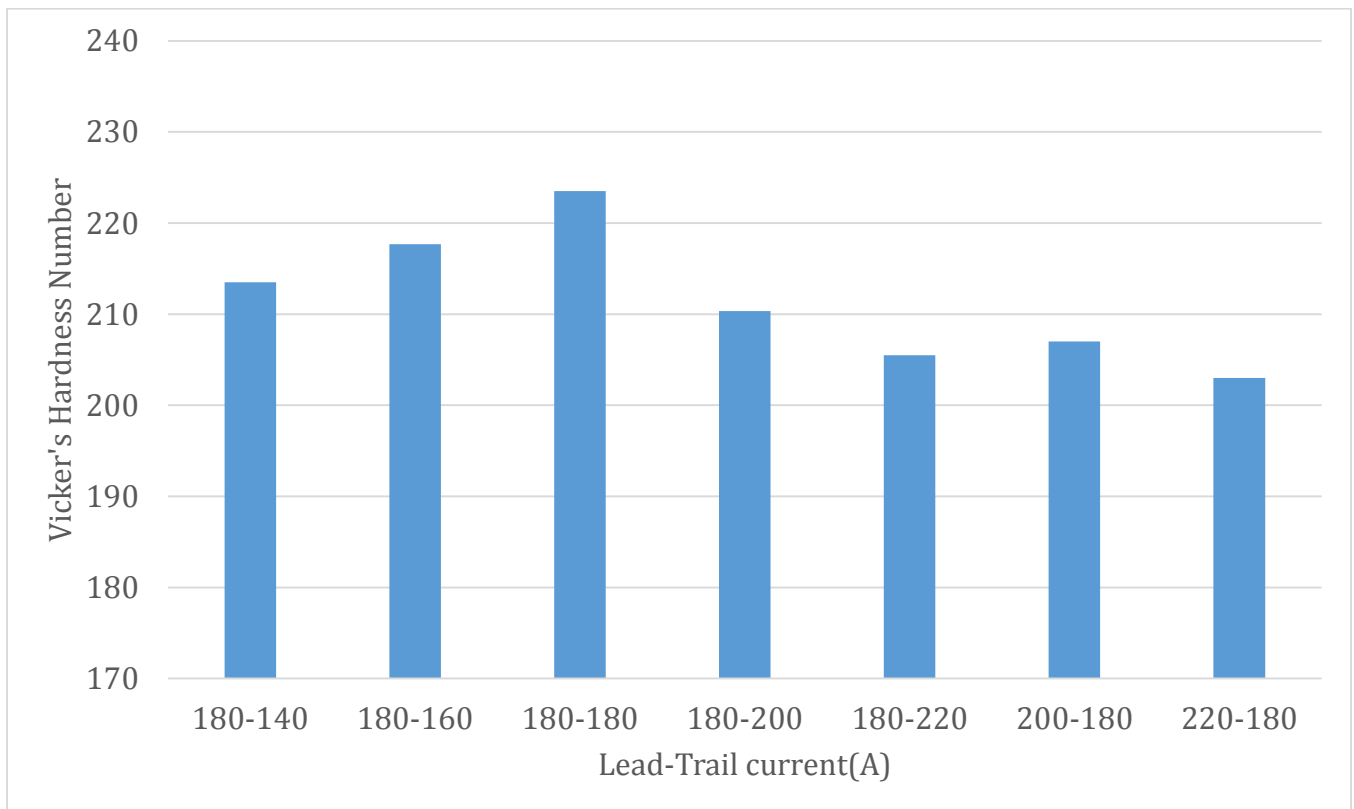


Figure 29–HAZ Hardness of dissimilar lead and trail current for 0.8-0.8mm wire diameter combination.

trail current. This shows that the HAZ Hardness of material is very much dependent on the stability of the arc.

The Figures (30 and 31) depict the bar chart of the set of experiments done with equal and unequal currents in lead and trail in which wire diameter combinations are correspondingly 0.8-1.2mm and 1.2-0.8mm. From the Figures (30 and 31) it can be observed that for the higher difference of Lead and trail the HAZ Hardness attains the least value. This shows that the higher stability of the arc lesser the value of HAZ Hardness is.

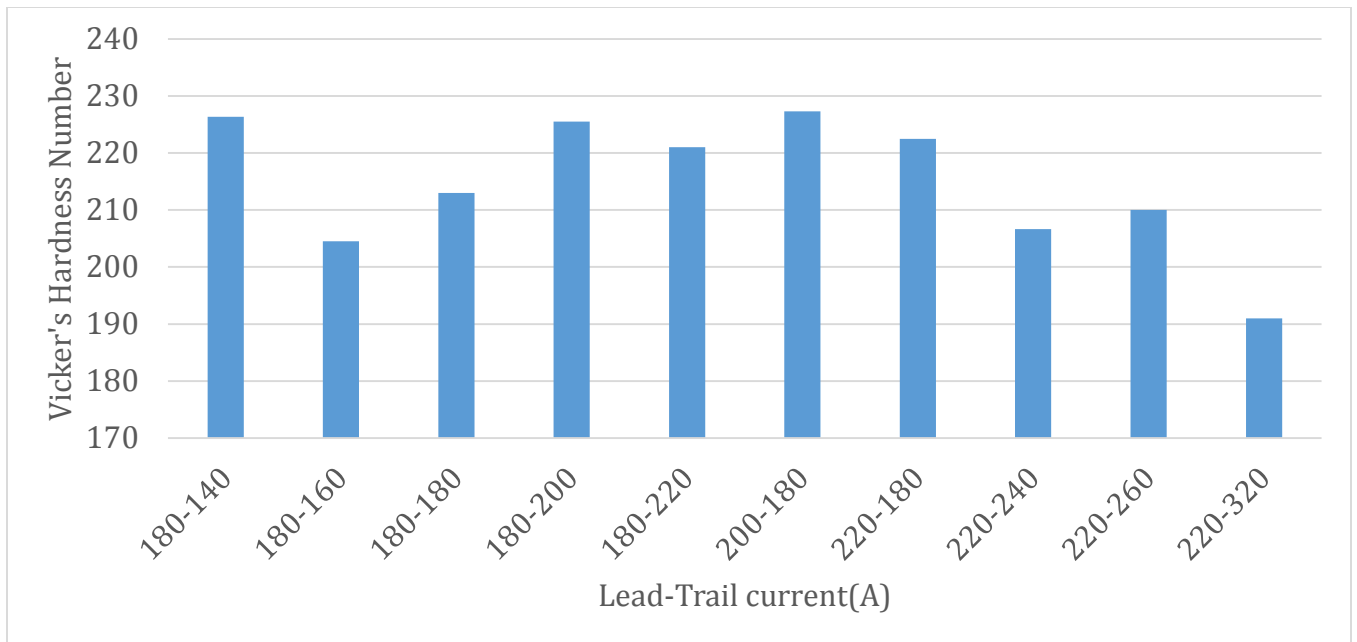


Figure 30–HAZ Hardness for 0.8-1.2mm wire diameter combination and dissimilar current.

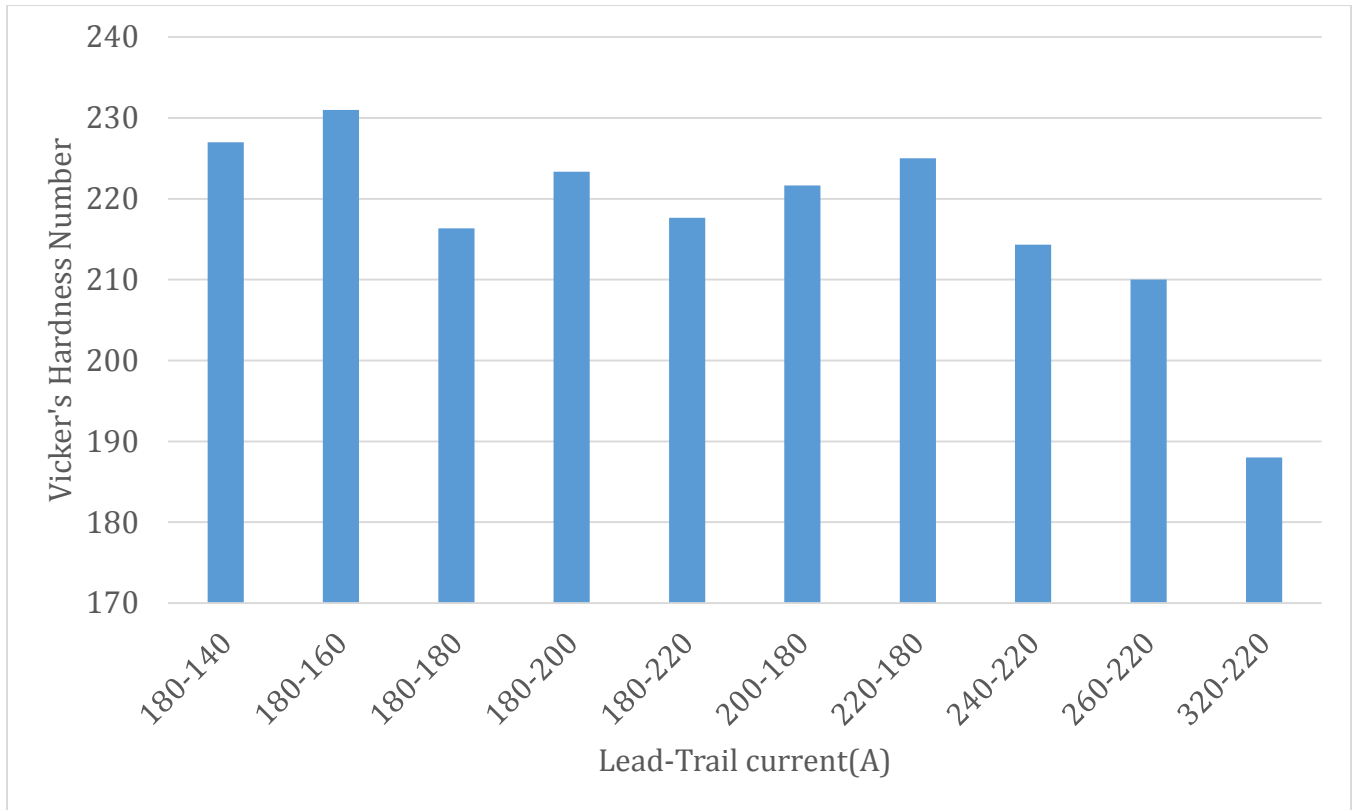


Figure 31–HAZ Hardness for 1.2-0.8mm wire diameter combination and dissimilar current.

6.2.2 HAZ Hardness analysis of equal current condition and different wire diameter combination:

The Figures (32, 33 and 34) show the bar chart of the HAZ Hardness for the set of experiments given in the Table 6. In these experiments the lead and trail current have been kept equal. The experiments have been conducted for different wire diameter combinations of the lead and trail which are 0.8-0.8mm, 1.2-0.8mm and 0.8-1.2mm. From the graphs shown in the Figures it can be observe that for higher current value the HAZ Hardness is comparatively smaller than the lower current value. Since due to the higher current there is a slight increase in the stability of the arc in the welding and along with that the proper heating also causing the reduction in the hardness.

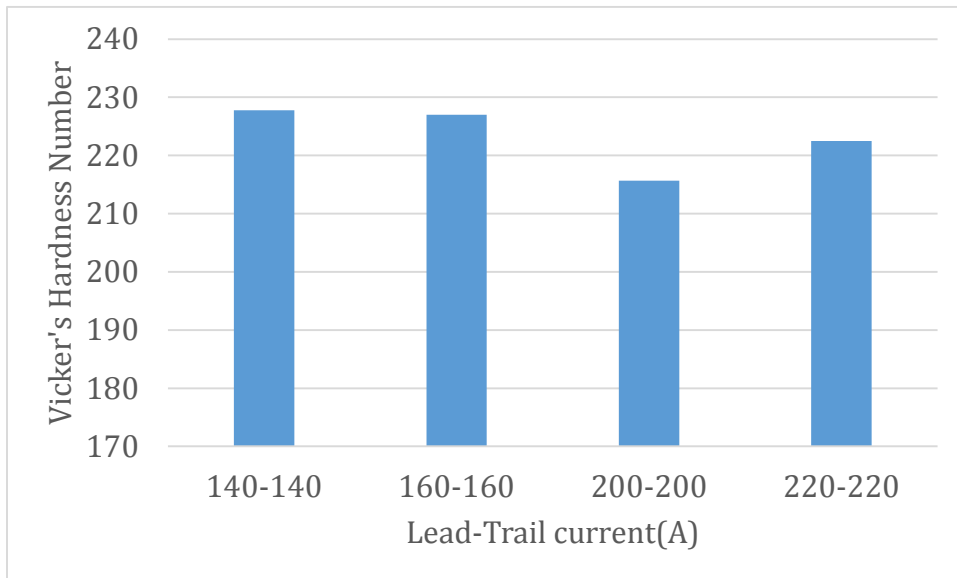


Figure 32–HAZ Hardness of equal current condition with 0.8-0.8mm wire diameter combination.

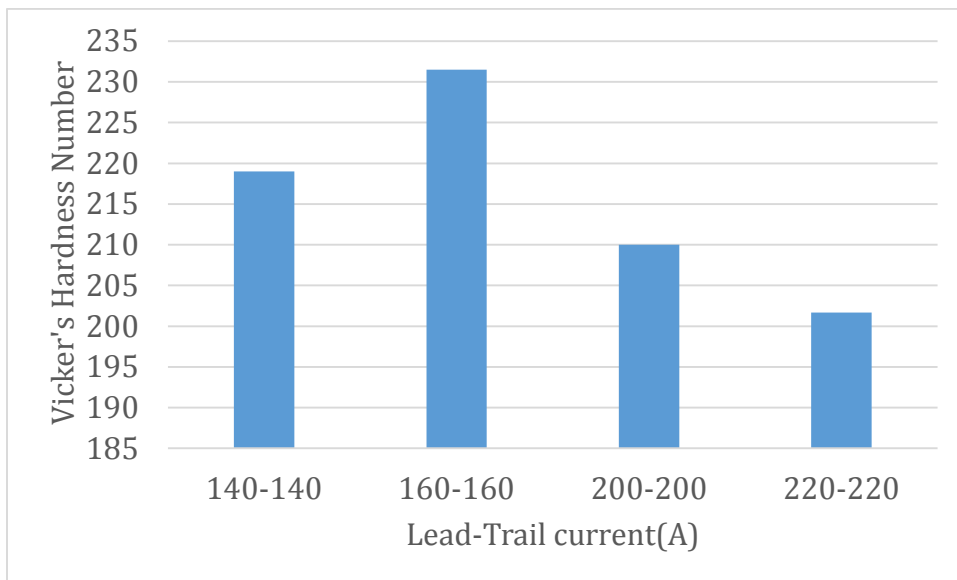


Figure 33–HAZ Hardness of equal current condition with 1.2-0.8mm wire diameter combination.

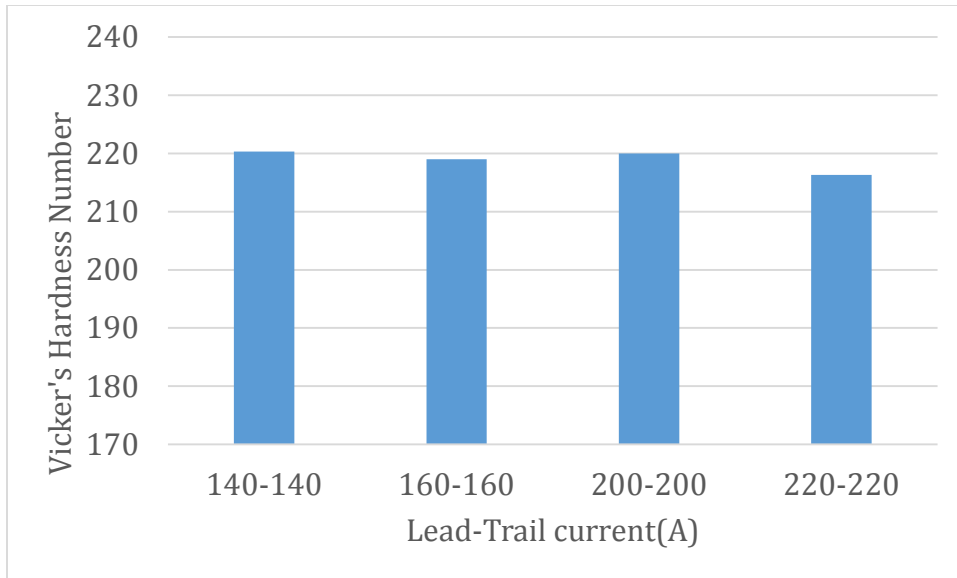


Figure 34–HAZ Hardness of equal current condition with 0.8-1.2mm wire diameter combination.

6.3 Aspect ratio (P/W) analysis:

It is the ratio of depth of penetration and width of weld bead. With increase in arc current the depth of penetration increases but for the same voltage condition if the current decreases then the depth of the penetration of arc decreases and width increases. But if the arc is unstable then due to flaring of arc there is an effect on the depth of penetration and the width of the weld.

From the trend line in Figure 35, it can be observed that with the increase in the difference of the lead and trail current density the aspect ratio increases. Whereas for the zero value of the difference between the current densities there is a least value of the aspect ratio. This shows that stability has an effect on the aspect ratio in twin wire gas metal arc welding. With increase in stability the aspect ratio increases and vice versa.

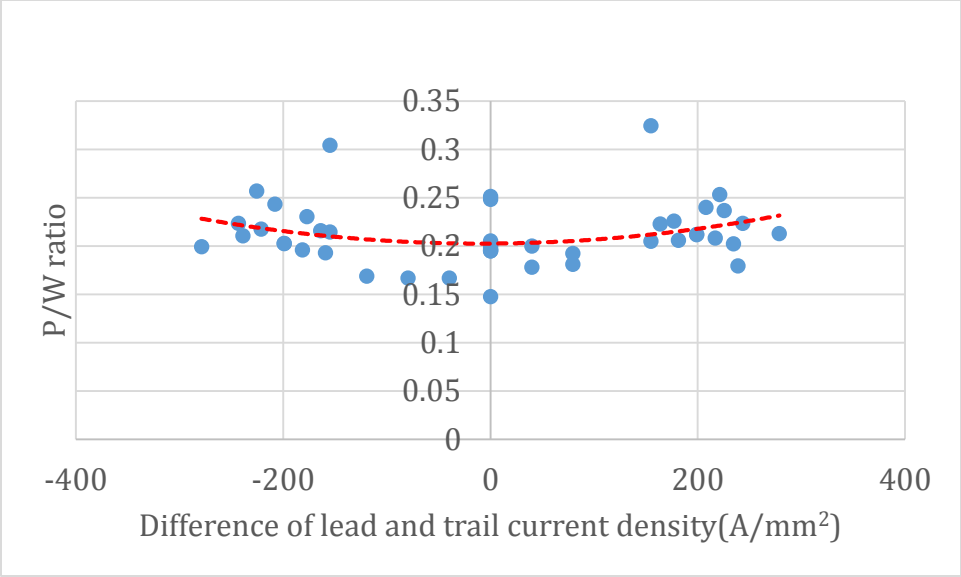


Figure 35-P/W ratio v/s current density difference graph.

Chapter 7

Conclusion and Future work

7.0 Overview

This section contains two parts. The first part is the conclusion of the work and the last part deals with the possible future work.

7.1 Conclusion

There are following conclusions of the results and discussions which have been done in the chapter6:

- In the case of similar wire diameter combination if the lead current is equal to the trail current then the arc instability will be maximum. But in the case of dissimilar currents, with the increase in the difference of lead and trail current the instability decreases. If lead current is more than the trail current with higher current-difference then the stability will be maximum.
- In the case of dissimilar wire diameter combination, with the increase in the difference of lead and trail current density the stability increases. But when the lead current intensity is more than the trail current density with higher difference then stability will be more than the greater value of trail current density condition.
- If the arc is highly stable then the HAZ Hardness attains the least value. This shows that the arc stability improves the mechanical properties of the heat affected zone.
- For the equal current condition if we increase the current value then due to change in mode of molten metal transfer arc stability increases. This increase in arc stability has been verified with the hardness of HAZ of weld for each experimental condition.
- In the case of equal diameter and equal current the trail arc possesses more instability than the lead arc.

- In the dissimilar electrode diameter case, with the increases in current (where lead and trail current are equal) the arc stability increases more significantly than the similar diameter case.
- If the arc is more stable then it will lead to a higher aspect ratio in weld and vice versa.

7.2 Future works

There are many possibilities of experiments which can be done for the further improvement Of this work. There are following possibilities:

- The arc stability analysis can be done for the different welding speed condition.
- The in-time arc stability can be analyzed using WEE for smaller time period and it can be compared for the different cases. This will give a visualization about the time period of the instability in the arc for different experimental conditions.
- The study of arc stability can be done for different types of current combinations of lead and trail like pulse-continuous, continuous-pulse, continuous-continuous, AC-DC, DC-AC, AC-AC.
- The effect of different current combinations and arc stability on the other mechanical properties of weld like Residual stress, toughness, Yield stress and fracture strength can be studied.

REFERENCES

- [1] Ueyama, T., T. Ohnawa, M. Tanaka, and K. Nakata. "Effects of torch configuration and welding current on weld bead formation in high speed tandem pulsed gas metal arc welding of steel sheets." *Science and Technology of Welding & Joining* 10, no. 6 (2005): 750-759.
- [2] Patnaik, A.;Poondla, N.;Bathini, U.;Srivatsan, T.S. On the use of Gas Metal Arc Welding for Manufacturing Beams of Commercially Pure Titanium and a Titanium Alloy,*Materials and Manufacturing Processes*, 2011, 26 (2), 311–318.
- [3] Devakumaran, K.;Rajasekaran,N.;Ghosh, P.K. Process Characteristics of Inverter Type GMAW Power Source under Static and Dynamic Operating Conditions, *Materials and Manufacturing Processes*,2012,27 (12), 1450–1456.
- [4] Suban, M.; Tušek, J. Methods for the Determination of Arc Stability, *Journal of Materials Processing Technology*, 2003, 143–144, 430–437.
- [5] Asthon T., 1954, Twin-wire submerged arc welding, *Welding Journal*, Vol. 33(4), 350- 355.
- [6] Bhide, S. R., Michaleris, P., Posada, M., & DeLoach, J. (2006). Comparison of buckling distortion propensity for SAW, GMAW, and FSW. *Welding journal*, 85(9), 189-195.
- [7] Lassaline E., Zajaczkowski B. and North T.H., 1989, Narrow groove twin wire GMAW of high-strength steel, *Welding Journal*, Vol. 68(9), 53-58
- [8] Tušek, J. (2000). Mathematical modeling of melting rate in twin-wire welding.*Journal of materials processing technology*, 100(1), 250-256.
- [9] Sharma, A., Arora, N., & Mishra, B. K. (2008). Mathematical modeling of flux consumption during twin-wire welding. *The International Journal of Advanced Manufacturing Technology*, 38(11-12), 1114-1124.
- [10] Sharma, A., Chaudhary, A. K., Arora, N., & Mishra, B. K. (2009). Estimation of heat source model parameters for twin-wire submerged arc welding. *The*

- international journal of advanced manufacturing technology, 45(11-12), 1096-1103.
- [11] Kiran D.V., Basu B., Shah A.K., Mishra S., and De A., 2011, Three-dimensional Heat Transfer Analysis of Two Wire Tandem Submerged Arc Welding, ISIJ International, Vol. 51 (5), 793–798.
- [12] Ma, G., & Zhang, Y. (2012). A novel DE-GMAW method to weld steel tubes on simplified condition. The International Journal of Advanced Manufacturing Technology, 63(1-4), 147-153.
- [13] Wei, H. L., Li, H., Yang, L. J., & Gao , Y. (2013). Consumable double electrode with a single arc GMAW. The International Journal of Advanced Manufacturing Technology, 68(5-8), 1539-1550.
- [14] FANG, C. F., MENG, X. H., HU, Q. X., WANG, F. J., He, R. E. N., WANG, H. S., ... & Ming, M. A. O. (2012). TANDEM and GMAW twin wire welding of Q690 steel used in hydraulic support. Journal of Iron and Steel Research, International, 19(5), 79-85.
- [15] Wang, Z. Z., & Zhang, Y. M. (2007). Image processing algorithm for automated monitoring of metal transfer in double-electrode GMAW. Measurement Science and Technology, 18(7), 2048
- [16] Li, K., & Zhang, Y. (2007). Metal transfer in double-electrode gas metal arc welding. Journal of Manufacturing Science and Engineering, 129(6), 991-999.
- [17] Li, K., & Zhang, Y. (2010). Interval model control of consumable double-electrode gas metal arc welding process. Automation Science and Engineering, IEEE Transactions on, 7(4), 826-839.
- [18] Wu, C. S., Hu, Z. H., & Zhong, L. M. (2012). Prevention of humping bead associated with high welding speed by double-electrode gas metal arc welding. The International Journal of Advanced Manufacturing Technology, 63(5-8), 573-581
- [19] Estefen, S. F., Gurova, T., Werneck, D., & Leontiev, A. (2012). Welding stress relaxation effect in butt-jointed steel plates. Marine Structures, 29(1), 211-225.

- [20] Meng, Q.G.; Fang H.Y.; Yang, J.G.; Ji, S.D. Analysis of Temperature and Stress Field in Al Alloys Twin-Wire Welding, *Theoretical and Applied Fracture Mechanics*, 2005, 44, 178-186.
- [21] Motta, M.F.; Dutra, J.C. Effects of the Variables of the Double Wire MIG/MAG Process with Insulated Potentials on the Weld Bead Geometry, *Welding International*, 2006, Vol. 20(10), 785-793.
- [22] Han B., Qu S.Y., and Zou Z.D., 2007, Arc phenomenon and core wire fusion in twin electrode single arc welding, *Science and Technology of Welding and Joining*, Vol. 12, 94-99
- [23] Ye, Dingjian, Xueming Hua, and Yixiong Wu. "Arc Interference Behavior during Twin Wire Gas Metal Arc Welding Process." *Advances in Materials Science and Engineering 2013* (2013).
- [24] Li, X., Li, Q., He, K., & Khalila, A. H. (2012). Arc Stability Analysis of Square Wave Alternating Current Submerged Arc Welding Based on Wavelet Energy Entropy. *Journal of Convergence Information Technology*, 7(22).
- [25] Moinuddin, S. Q., & Sharma, A. (2015). Arc stability and its impact on weld properties and microstructure in anti-phase synchronised synergic-pulsed twin-wire gas metal arc welding. *Materials & Design*, 67, 293-302.
- [26] Azar, Amin S., Neil Woodward, Hans Fostervoll, and Odd M. Akselsen. "Statistical analysis of the arc behavior in dry hyperbaric GMA welding from 1 to 250bar." *Journal of Materials Processing Technology* 212, no. 1 (2012): 211-219.
- [27] Weite Wu, Influence of vibration frequency on solidification of weldments, *Scripta Materialia*, Volume 42, Issue 7, 17 March 2000, Pages 661-665, ISSN 1359-6462.
- [28] Qinghua Lu, Ligong Chen, Chunzhen Ni, Improving welded valve quality by vibratory weld conditioning, *Materials Science and Engineering: A*, Volume 457, Issues 1-2, 25 May 2007, Pages 246-253, ISSN 0921-5093, <http://dx.doi.org/10.1016/j.msea.2006.12.120>.
- [29] R. Dehmlaei, M. Shamanian, A. Kermanpur, Effect of electromagnetic vibration on the unmixed zone formation in 25Cr-35Ni heat resistant steel/Alloy

- 800 dissimilar welds, *Materials Characterization*, Volume 59, Issue 12, December 2008, Pages 1814-1817, ISSN 1044-5803
- [30] Takehiko Watanabe, Masataka Shiroki, Atsushi Yanagisawa, Tomohiro Sasaki, Improvement of mechanical properties of ferritic stainless steel weld metal by ultrasonic vibration, *Journal of Materials Processing Technology*, Volume 210, Issue 12, 1 September 2010, Pages 1646-1651, ISSN 0924-0136,
- [31] Suban, M., & Tušek, J. (2001). Dependence of melting rate in MIG/MAG welding on the type of shielding gas used. *Journal of Materials Processing Technology*, 119(1), 185-192.
- [32] Murphy, A. B. (2013). Influence of metal vapour on arc temperatures in gas-metal arc welding: convection versus radiation. *Journal of Physics D: Applied Physics*, 46(22), 224004.
- [33] Pal, K.; Pal, S.K. Monitoring of Weld Penetration using Arc Acoustics, *Materials and Manufacturing Processes*, 2011, 26 (5), 684–693.
- [34] de Meneses, V. A., Gomes, J. F. P., & Scotti, A. (2014). The effect of metal transfer stability (spattering) on fume generation, morphology and composition in short-circuit MAG welding. *Journal of Materials Processing Technology*, 214(7), 1388-1397.
- [35] Ganesan R, Das TK, Venkataraman V (2004) Wavelet-based multiscale statistical process monitoring: a literature review. *IEEE Trans* 36:787–806
- [36] Liang S, Hecker R, Landers R (2004) Machining process monitoring and control: the state-of-the-art. *ASME J Manuf Sci Eng* 126(2):297–310
- [37] Toñshoff H, Wulfsberg J, Kals H, König W (1988) Developments and trends in monitoring and control of machining processes. *Ann CIRP* 37(2):611–622
- [38] Byrne G, Dornfeld D, Inasaki I, Ketteler G, König W, Teti R (1996) Tool condition monitoring (TCM) – the status of research and industrial application. *Ann CIRP* 44(2):541–567
- [39] Gu S, Ni J, Yuan J (2002) Non-stationary signal analysis and transient machining process condition monitoring. *Int J Mach Tools Manuf* 42:41–51
- [40] . Padovese LR (2004) Hybrid time-frequency methods for non-stationary mechanical signal analysis, *Mech Syst Signal Process* 18(5):1047–1064

- [41] Shi DF, Tsung F, Unsworth PJ (2004) Adaptive time-frequency decomposition for transient vibration monitoring of rotating machinery. *Mech Syst Signal Process* 18(1):127–141
- [42] Chui CK (1992) *An introduction to wavelets*. Academic, New York
- [43] Gabor D (1946) Theory of communication. *J Inst Electr Eng* 93:429–457
- [44] Cohen L (1989) Time-frequency distributions – a review. *Proc IEEE* 77(7):941–981
- [45] Zhou SY, Sun BC, Shi JJ (2006) An SPC monitoring system for cycle-based waveform signals using haar transform. *IEEE Trans Automat Sci Eng* 3(1):60–72
- [46] Kim JS, Lee JH, Kim JH, Baek J, Kim SS (2010) Fault detection of cycle-based signals using wavelet transform in FAB processes. *Int J Precision Eng Manuf* 11(2):237–246
- [47] Rafiee J, Rafiee MA, Tse PW (2010) Application of mother wavelet functions for automatic gear bearing fault diagnosis. *Expert Syst Appl* 37:4568–4579
- [48] Gao R, Yan R (2006) Non-stationary signal processing for bearing health monitoring. *Int J ManufRes* 1(1):18–40
- [49] Shakher C, Ishtiaque SM, Singh SK, Zaidi HN (2004) Application of wavelet transform in Characterization of fabric texture. *J Text Inst* 95(1–6):107–120
- [50] Erlebacher G, Yuen DA (2004) A wavelet toolkit for visualization and analysis of large data sets in earthquake research. *Pure Appl Geophys* 161(11–12):2215–2229
- [51] Lin J, Qu L (2000) Feature extraction based on Morlet wavelet and its application for mechanical fault diagnosis. *J Sound Vib* 234(1):135–148
- [52] Gao, R. X., & Yan, R. (2010). *Wavelets: Theory and applications for manufacturing*. Springer Science & Business Media.
- [53] Zhang, Chunguo, Xiaozhi Hu, and Pengmin Lu. "Fatigue and hardness effects of a thin buffer layer on the heat affected zone of a weld repaired Bisplate80." *Journal of Materials Processing Technology* 212.2 (2012): 393-401.
- [54] Li, Xuejun, et al. "Arc Stability Analysis of Square Wave Alternating Current Submerged Arc Welding Based on Wavelet Energy Entropy." *Journal of Convergence Information Technology* 7.22 (2012).

